2011

Real-time Fault Diagnosis of Automotive Electrical Power Generation and Storage System

Luis Farfan-Ramos
Wright State University

REAL-TIME FAULT DIAGNOSIS OF AUTOMOTIVE ELECTRICAL POWER GENERATION AND STORAGE SYSTEM

A thesis submitted in partial fulfillment
of the requirements for the degree of
Master of Science in Engineering

By

LUIS FARFAN-RAMOS
B.S., Wright State University, 2009

2011
Wright State University

WRIGHT STATE UNIVERSITY

SCHOOL OF GRADUATE STUDIES

April 8, 2011

I HERBY RECOMMEND THAT THE THESIS PREPARED UNDER MY SUPERVISION BY Luis Farfan-Ramos ENTITLED Real-Time Fault Diagnosis of Automotive Power Generation and Storage System BE ACCEPTED IN PARTIAL FULFILLMENT OF THE REQUIREMENTS FOR THE DEGREE OF Master of Science in Engineering.

_____

Xiaodong Zhang, Ph.D.
Thesis Director

_____

Kefu Xue, Ph.D.
Chair, Department of Electrical Engineering
College of Engineering and Computer Science

Committee on
Final Examination

_____

Xiaodong Zhang, Ph.D.

_____

Kuldip S. Rattan, Ph.D.

_____

Marian Kazimierczuk, Ph.D.

_____

Andrew Hsu, Ph.D.
Dean, School of Graduate Studies

ABSTRACT

Farfan-Ramos, Luis. M.S.E., Department of Electrical Engineering, Wright State University, 2011. Real-time Fault Diagnosis of Automotive Electrical Power Generation and Storage System.

Automobiles depend more and more on electric power. Analysis of warranty data by automotive OEMs shows that faults in the automotive electrical power generation and storage (EPGS) system are often misdiagnosed. Therefore, monitoring of the state of health (SOH) of the automotive EPGS system is vital for early and correct diagnosis of faults in it, ensuring a reliable supply of electric power to the vehicle and reducing maintenance costs. In this research project, a model-based SOH monitoring method for the EPGS system is developed without the requirement of an alternator current sensor. A model representing the dynamic relationship between the battery current and the alternator filed duty voltage cycle is presented. An important model parameter that characterizes the current generation efficiency of the alternator system is adaptively estimated by using a recursive least square algorithm. Based on fault modes and effect analysis, a model-based fault detection and isolation decision scheme is developed for the EPGS system faults under consideration. The SOH monitoring method has been implemented using an EPGS system experimental test bench at GM R&D Center. Real-time evaluation results have shown its effectiveness and robustness.

TABLE OF CONTENTS

Page

LIST OF FIGURES

Figure Page

LIST OF TABLES

Table Page

AKNOWLEDGEMENT

It is a pleasure to thank those who with their help and guidance made this thesis possible.

First and foremost, I want to thank Dr. Xiaodong (Frank) Zhang, professor at Wright State University's Department of Electrical Engineering, who invited me to participate in his research on fault diagnosis of automotive electrical systems among other innovative research projects.

I also want to thank Dr. Yilu Zhang, researcher at General Motors Research & Development Center in Warren, Michigan, who made possible the sponsorship of this research project and gave us access to the laboratory equipment needed for the development and validation of the proposed fault diagnosis method.

Last but not least, I want to thank Stephen Nawrocki, engineer at General Motors Research & Development Center in Warren, Michigan, who helped me on the data collection and algorithm validation tasks throughout most of the project.

I. INTRODUCTION

Automobiles depend more and more on electric power [5], [10], which is due to the growing number of electrical systems needed to meet consumer demands and regulations. For instance, anti-lock braking and stability control systems for enhanced performance and safety; seat heating, audio, and video systems for added comfort. Furthermore, many mechanical systems are gradually being replaced by electrical counterparts. For example, hybrid electric propulsion systems instead of pure internal combustion engine (ICE) based propulsion systems, and drive-by-wire systems instead of conventional hydraulic steering systems.

Yet, analysis of warranty data carried out by automotive original equipment manufacturers (OEMs) shows that faults in the automotive electric power generation and storage (EPGS) system are often misdiagnosed. For instance, a faulty alternator current rectifier or an improperly tensed driving belt is often diagnosed as a faulty battery. This leads to the unnecessary stock, purchase, and replacement of automotive parts, which not only translates into additional maintenance costs for automobile suppliers and customers, but also into reduced vehicle reliability.

Therefore, monitoring of the state of health (SOH) of the automotive EPGS system is vital for early and correct diagnosis of faults in it, ensuring a reliable supply of electrical power to the vehicle and reducing maintenance costs.

In the fault diagnosis literature, there has been significant research and development of model-based fault detection and isolation (FDI) schemes [1], [4], [6], [8], and many robust on-board state-of-health (SOH) monitoring technologies for the automotive EPGS system have been proposed [3], [9], [10], [11].

However, the automotive EPGS system is very complex. For instance, the rotor-stator system in the alternator has a highly nonlinear dynamics and the diode bridge rectifier has a discontinuous switching behavior. In addition, the components of the EPGS system come from different suppliers, which makes difficult to establish a unique, accurate model of the system; automotive electronic control units (ECUs) have limited computing power available because they already execute many other diagnosis tasks; and more importantly, in actual automotive EPGS systems, there are limited sensor measurements. All of which make the diagnosis of faults in the EPGS system challenging.

In previous collaborative research [12], the design of robust SOH monitoring algorithms for automotive batteries was already considered. The other important component of the EPGS system is the alternator. In [13] and [14], a parity-relation based fault diagnostic method was developed for the alternator by using principal/minor component analysis techniques. However, a key assumption made in [12], [13], and [14] is that the alternator output current is measured, which is not always the case. In most GM vehicles, an alternator current sensor is rarely installed for the sake of cost saving.

In this research project, a real-time model-based SOH monitoring method for the EPGS system without the requirement of an alternator current sensor is developed.

Based on the operating principle of the EPGS system, a mathematical model representing the dynamic relationship between the battery current and the alternator filed voltage duty cycle is presented. An important model parameter characterizing the current generation efficiency of the alternator system is estimated on-line by using a recursive least square algorithm. According to fault modes and effect analysis, a model-based fault detection and isolation decision scheme is developed for the EPGS system faults under consideration.

The proposed model-based SOH monitoring method has been implemented using an EPGS system experimental test bench at General Motors Research & Development Center. Real-time evaluation results have shown the robustness and effectiveness of the algorithm.

This thesis report is organized as follows. In Section II, an overview of the different fault diagnosis techniques, with focus on model-based methods, is presented. In Section III, the EPGS system and faults under consideration are introduced. Section IV describes the model-based SOH monitoring algorithm, including the diagnosis residual generation and residual evaluation tasks. The real-time implementation of the SOH monitoring method is detailed in Section V. In Section VI, several representative case studies are shown to illustrate the effectiveness and robustness of the algorithm. Finally, in Section VII, some concluding remarks and directions for future research work are presented.

II. MODEL-BASED FAULT DIAGNOSIS

In technical processes, fault diagnosis essentially comprises the tasks of fault detection and isolation (FDI). The *fault detection* task reports the occurrence of any fault within the system. Then, the *fault isolation* task determines the exact location of the fault(s). These tasks can be carried out using hardware or model/software based techniques [1], [4], [6], [8]. However, as will be shown, model-based methods are more reliable and yield greater information about the state of health (SOH) of the system. Before proceeding, it is important to distinguish between fault and failure.

A *fault* is the deviation of a property of a system from its nominal (or acceptable) value changing the system's input-to-output characteristic to the point of not allowing it to function properly; for example, a sensor bias, blocking of an actuator, fluid leaks, etc.

A *failure*, on the other hand, is the permanent or total inability of a system to perform a function as a consequence of the advanced condition of one or more faults.

The simplest hardware-based technique to detect faults is *limit checking*. If a signal in the system goes beyond its normal limits, an alarm is activated. However, this method has several drawbacks. First, not all signals of interest may be accessible and/or measurable; for instance, the gas pressure in a jet engine combustion chamber, where the temperature is very high. Second, usually, signal limits (thresholds) will have large enough tolerances to avoid false alarms. Therefore, a fault either must be abrupt and large

o must be growing for a long period of time before it can be detected. On the other hand, false alarms may be triggered if the system's operating point is changed. As a result, multiple alarms being triggered at the same time ("alarm showers") are very likely. Moreover, by the time a fault is detected, parts of the system may have already reached their failure point, compromising the availability and, more importantly, the safety of the system and its surroundings. Hence, limit checking allows the detection of failures rather than faults.

In safety-critical systems such aircrafts and nuclear plants, typically, faults are detected by incorporating *hardware redundancy*. In this approach, additional sensors, actuators, and other plant components are placed and run in parallel with the primary components. If the difference between the outputs of a primary component and its redundant counterpart is significantly large, the simplest decision is to declare that the primary component is faulty. The advantages of this method are its high reliability and direct fault isolation. In addition, in the event of a fault, the redundant component may take the place of the primary component, so the system continues functioning properly. The main drawback of this method is its high cost due to the additional hardware needed. Consequently, its usage is restricted to key components. In addition, it is not always implementable because of physical space constrains.

In view of this, in the early 1970s, inspired by the newly developed observer theory and the arrival of the microprocessor, the automatic control community started developing analytical, software-based methods for real-time fault diagnosis; an important example of which was the called "failure detection filter" by Bear and Jones. Nowadays, contributions also come from other research fields such as computer science and are

driven by the demand of safer processes not only from safety-critical industries such as the aircraft industry, but also from more consumer oriented industries such as the automotive industry. The most relevant analytical fault-diagnosis methods are based in signal models and process models.

Signal-model based fault diagnosis methods extract features from the system signals to detect and isolate faults. These methods can be classified in *time based* methods such as principal component analysis (PCA), which relies on the change of the correlation between the system signals as consequence of faults; and *frequency based* methods such as spectral analysis, which relies on the change of the frequency content in system signals due to faults, for instance, oscillations due to machine vibrations.

Process-model based fault diagnosis methods, also called analytical redundancy or software redundancy methods, make use of a mathematical description (model) of the of the input/output characteristics of the process (or plant), for instance, transfer functions, to generate estimations of system features, such as dynamic states, which then are compared with the features actually being observed to generate diagnosis *residuals*. If the model of the process is accurate enough, under normal operating conditions, all residuals should remain small, while under faulty conditions, at least one residual should become large, indicating the occurrence of a fault. Furthermore, the residuals are compared with threshold values to produce diagnosis *symptoms*, for instance, in binary form, which then may be looked up in a diagnosis table to isolate the fault. Alternatively, if no relations between faults and residuals are known, classifications methods such as pattern recognition might be used to detect and isolate the faults.

Process-model based fault diagnosis methods not only allow the diagnosis of faults without the need of redundant process components, but also the diagnosis of faults in inaccessible components, and the diagnosis of small faults in closed control loops. All without the need of additional sensors either, since, in most cases, the input and output signals of the process controller are sufficient for the generation of diagnosis residuals. In addition, the generation of the diagnosis residuals and the fault detection and isolation operations may be carried out in the same computer that hosts the process controller, with the only requirements of additional memory and processing power, if necessary.

Additionally, process-model based fault diagnosis methods also allow the estimation of the magnitude of the faults, formally called fault *identification*, which brings many benefits. For instance, *supervisory control* programs this information to reconfigure the process control algorithm and accommodate the faults, so the system continues operating safely. Systems of this type are called *fault tolerant*. Notice that supervisory control goes beyond *adaptive control*, in which the controller parameters are adjusted automatically to optimize the system response, but under the assumption that the process parameters have not changed, that is, assuming the system is not faulty. In addition, the estimation of the magnitude of the faults allows the early scheduling of maintenance procedures to further extend the efficiency and availability of the system.

The mathematical model of the process (or plant) can be obtained manually from measurements of its physical parameters or by using system identification techniques such as least squares algorithms. However, it is not always possible to model the process to a full extent and/or to a great level of accuracy. Therefore, process-model based fault

diagnosis algorithms need to be designed to be tolerant or *robust* to modeling uncertainties, which currently is a topic of extensive research.

In order to do design and evaluate the performance of a process-model based fault diagnosis algorithm, it is also be necessary to model the faults involved. There are two main types of faults: *additive faults*, which are seen as external signals entering the system and are mostly used to model biases in sensors; and *multiplicative faults*, which are used to model changes in the parameters of actuators and other system components. Furthermore, it is also necessary to model the incidence of the faults. For instance, faults can be *abrupt*, in which case they are modeled as stepwise signals; they can be *insipient*, in which case they are modeled as drift-like signals; or they can be *intermittent*, in which case they are modeled as signals with random occurrence.

There are three main process-model based fault diagnosis methods: the parity equation method (or parity space method), the observer method, and the parameter estimation method.

The *parity equation* based fault diagnosis method has the most straightforward implementation. The process model is fed with the same control signal as the actual process and run in parallel with it. Then, the outputs of both the model and the actual process are compared to generate a diagnosis residual. Alternatively, the diagnosis residual can be obtained by converting the process model into an error polynomial equation which is fed by the process input and output signals. Furthermore, in multivariable systems, the process model can be converted into state-space error equations in which the gain matrices are selected to suppress the effect of an input on a

specific residual and, hence, enhance the fault isolation capabilities of the algorithm. The parity equation based fault diagnosis method has shown to be simpler than the observer based method described next.

In the *observer* based fault diagnosis method, either the states of the process or the states if its outputs are estimated to generate diagnosis residuals. State observers allow the diagnosis of dynamic faults such as leaks. Output observers allow the diagnosis of faults in sensors and actuators without the need of computing the process states and independently of the unknown inputs. However, both observer based fault diagnosis techniques require precise knowledge of the process model matrices.

Finally, in the *parameter estimation* based fault diagnosis method, the process physical parameters, such as stiffness, damping, electrical resistance, and capacitance, are estimated and compared with their corresponding expected, normal parameters to generate the diagnosis residuals. The estimations are carried out using numerical optimization methods such as least squares algorithms and neural networks. These algorithms are based on the minimization of the output of an error equation, which is set up from the knowledge of the basic structure of the process model. The main advantage of this method is that it allows the estimation of parameters in nonlinear systems.

As will be shown, in this research project, the parameter estimation method via a least squares algorithm in recursive form is used to generate diagnosis residuals for the diagnosis of faults in the automotive EPGS system.

III. AUTOMOTIVE EPGS SYSTEM DESCRIPTION

In this section, the configuration of the automotive EPGS system is briefly described, and the effect of the faults under consideration is analyzed.

1. EPGS System Configuration

The automotive EPGS system is composed of an alternator, a battery, a belt-pulley system, and two electronic control units (ECUs): the engine control module (ECM) and the body control module (BCM) [2], [5]. The EPGS system supplies the electric power needed to drive the various electrical devices in the vehicle.

As shown in Figure 1, the *alternator* is primarily made up of stator windings, usually connected in a "Y" configuration, a three-phase diode bridge rectifier, a rotor winding with slip rings and brushes, a pulley attached to the rotor shaft, and a voltage regulator. The regulator applies a voltage signal to the rotor winding, which generates magnetic field around it. The internal combustion engine (ICE) drives the alternator's shaft through the *belt-pulley system*. When the rotor winding is turned, the rotating magnetic field induces an alternating current (AC) through the stator windings. The three-phase diode bridge rectifier converts the AC signal to direct current (DC), which is used to power the electrical systems in the vehicle and charge the battery.

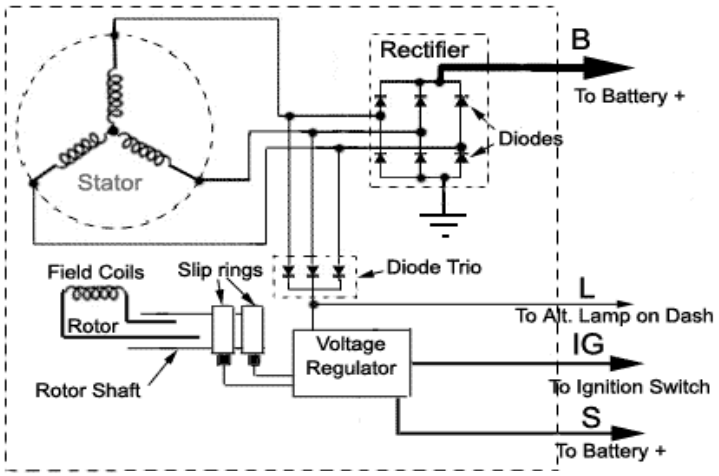

Figure 1: Configuration of the automotive alternator [2], [5].

The alternator output current is regulated to keep alternator output voltage approximately constant. More exactly, the voltage signal (or field voltage) that the regulator applies to the rotor winding is a pulse wide modulated (PWM) signal. The regulator senses the alternator output voltage and adjusts the duty cycle of the PWM voltage signal, which in turn changes the intensity of the magnetic field produced by the rotor winding; hence, controlling the magnitude of the alternator output current.

In parallel to the alternator, the *battery* provides electric power to the vehicle, in the following situations [2], [5]:

- When the engine is not running. For instance, to power the electric motor that starts (cranks) the engine.
- When the electric current produced by the alternator is not sufficient to properly power the vehicle's electrical load. For instance, when multiple electric devices (e.g., air conditioning fan, lights, radio) are on while the engine speed is low (e.g., engine idle), or when the alternator is deteriorated.

- During sudden electrical load changes since it takes some time for the alternator to respond to this changes. If the electrical load has increased, the battery sources the additional current needed. If the electrical load has decreased, the battery sinks the excess current produced by the alternator. In either case, the battery helps maintaining the voltage across the load constant.

The *electronic control units,* i.e., the ECM and the BCM, among many other tasks, carry out electric power management operations. For example, based on the state-of-charge (SOC) of the battery, they adjust the reference voltage of the regulator in the alternator; hence, controlling the charging voltage of the battery in order to maximize the life of the battery and the efficiency of the alternator.

2. Alternator Related Faults

In order to guarantee a reliable supply of electric power to the vehicle, faults in the EPGS system need to be diagnosed correctly and as early as possible. In previous collaborative work [12], several battery state-of-health (SOH) monitoring algorithms were developed. Like in previous collaborative research [13], [14], in this research project, the objective is to be able to diagnose faults in alternator system (i.e., the alternator plus belt-pulley system), but this time without the requirement of an alternator output current sensor.

Based on analysis of warranty data carried out by automotive original equipment manufacturers (OEMs), it was determined that the most common types of faults related to the alternator system are:

- *Diode short*, in which case one or more diodes of the three-phase diode bridge rectifier permanently conducts current. As a result, the alternator output current becomes unstable with large magnitudes of noise, which gradually damages the battery. A diode short is often caused by excessive voltage across the diode due to sudden, large changes in the vehicle's electrical load.

- *Belt slip*, in which case the rotational speed of the alternator shaft drops, sometimes to the point of becoming less than the rotational speed of the engine shaft (the nominal alternator to engine speed ratio is usually three). As a result, the current generated by the alternator drops. The regulator increases the duty cycle of the PWM field voltage signal in an attempt to boost the current generated by the alternator, but often the field voltage reaches saturation, and the battery starts sourcing current to compensate for the alternator current lost. Eventually, the battery becomes drained, leaving the vehicle inoperative. Belt slip occurs due to improper tensioning of the belt or due to normal wear of the belt. It usually manifests when the engine speed is low and the electrical load becomes high, in which case a larger torque about the alternator shaft is needed to keep it rotating at the same speed, but since the belt does not have a enough grip on the engine and alternator pulleys, it slips.

- *Regulator fault*, which occurs when the voltage regulator loses its signal control capabilities. More exactly, the duty cycle of the PWM field voltage signal remains fixed at an arbitrary value. Consequently, the alternator output current depends solely on the engine speed, and the battery may get damaged due to an overcharge or depleted due to insufficient charging. In either case, the vehicle would eventually become inoperative.

As pointed out in previous collaborative research [13], [14], the regulator fault can be relatively easily diagnosed by measuring the difference between battery voltage and the regulator reference voltage specified by the alternator L-terminal. Therefore, this research project is centered on the diagnosis of belt slip and diode short faults.

IV. TECHNICAL APPROACH

In this section, the model-based SOH monitoring method for the EPGS system is specified. First, the development of a mathematical model which characterizes the dynamic relationship between battery current and alternator filed duty cycle is described. Then, the model-based SOH monitoring method is detailed, including the diagnosis residual generation and residual evaluation tasks, respectively.

1. Model Development

The SOH monitoring method is developed based on the observation that the change in alternator output current is approximately directly proportional the change in the duty cycle of the alternator PWM field voltage signal. This important feature of alternator physical dynamics is illustrated in Figure 2, Figure 3, and Figure 4. Specifically, Figure 2 shows the alternator current (i.e., I_{alt}), filed voltage duty cycle (i.e., V_f), and the alternator-to-engine RPM ratio for a set of data collected at 800 RPM. An enlarged plot of the first transient is given in Figure 3 to illustrate the behavior of the alternator current and the filed voltage duty cycle during a transient period. Finally, the signals corresponding to the transients are extracted and given in Figure 4. From the third plot, we can clearly see a linear relationship between change in alternator current (i.e., ΔI_{alt}) and the change in field voltage (i.e., ΔV_f), where ΔI_{alt} and ΔV_f are defined as the difference between the instantaneous alternator current and instantaneous field voltage

values during the transient with respect to their corresponding steady-state values prior to the transient.

This linear relationship between ΔI_{alt} and ΔV_f can be described by:

$$\Delta I_{alt} = \eta * \Delta V_f + \beta \tag{1}$$

where the parameter β represents the alternator-current steady-state value prior to the transient, and more importantly, the parameter η characterizes the electric-current-generation efficiency of the alternator system (belt-pulley-alternator system) for certain changes in field voltage, which is also an indicator of state of health of the EPGS system. However, a major challenge in automotive EPGS system diagnostics/prognostics is that alternator current signal is rarely measured in production vehicles for the sake of cost saving. Therefore, the ΔI_{alt} signal cannot be obtained directly. However, as will be shown, it can be estimated from measurements of battery current signal.

Based on EPGS system dynamics, we have:

$$\begin{aligned} \Delta I_{alt} &= I_{alt} - I_{altss} \\ I_{alt} &= I_{bat} + I_{load} \end{aligned} \tag{2}$$

where I_{altss} is the steady-state alternator current before the transient occurs, and I_{alt}, I_{bat}, and I_{load} are the alternator current, battery current, and electrical load current signals during a transient, respectively. Combing the two equations in (2) yields:

$$\Delta I_{alt} = I_{bat} + I_{load} - I_{altss}\,. \tag{3}$$

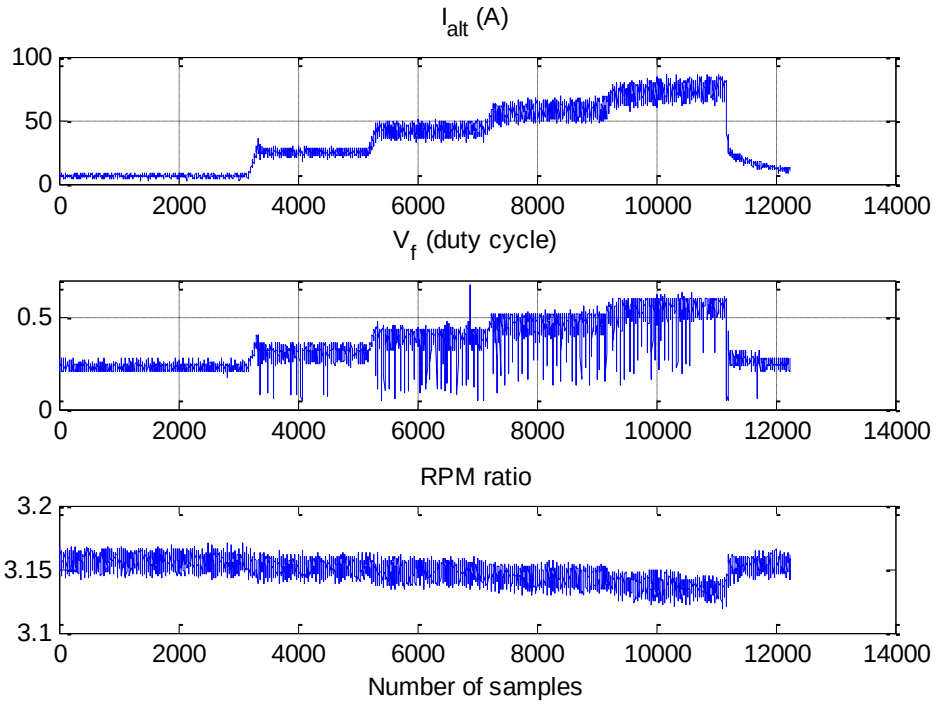

Figure 2: Alternator current signal, field voltage duty cycle, and alternator-to-engine RPM ratio.

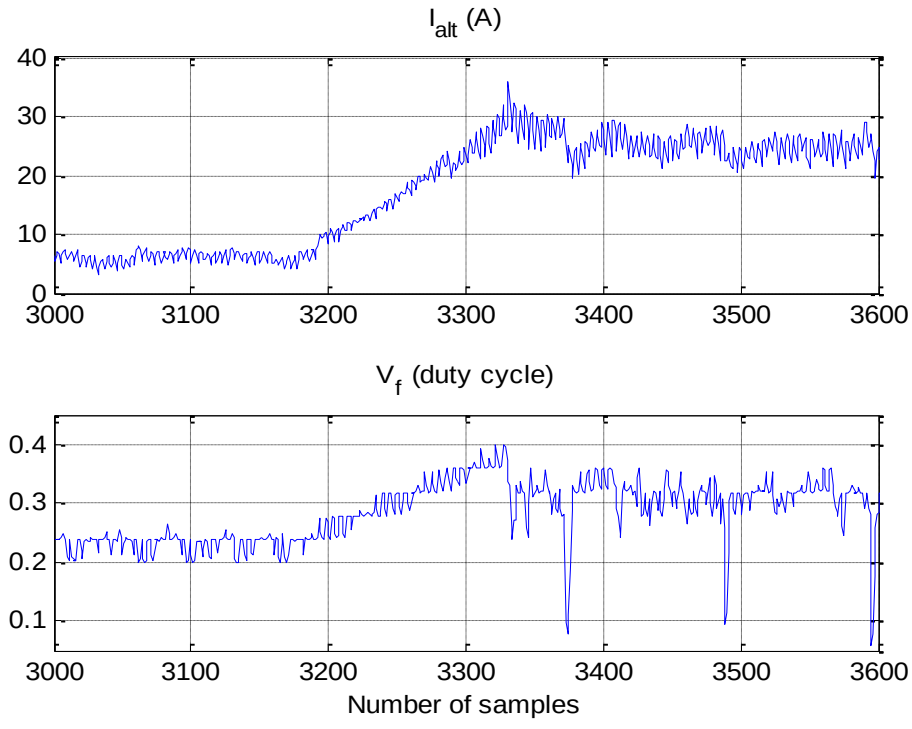

Figure 3: Enlarged plot of one transient of the alternator signals given in Figure 2.

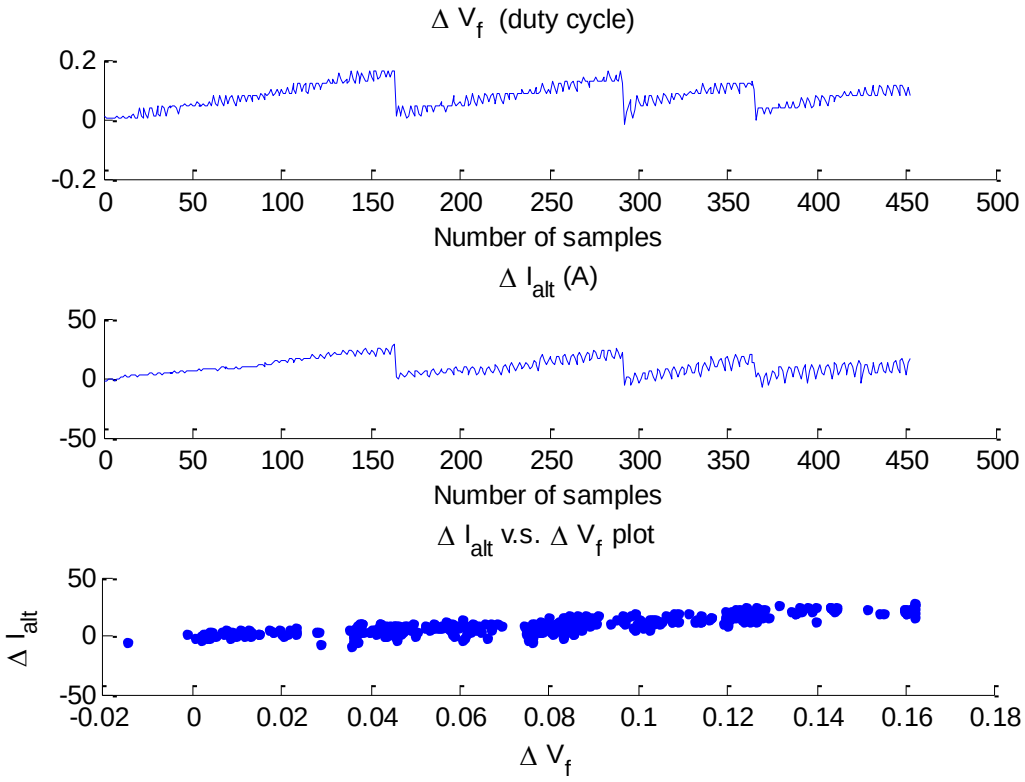

Figure 4: Relationship between $\Delta \boldsymbol{I_{alt}}$ and $\Delta \boldsymbol{V_f}$.

Now, substituting (1) into (3) yields:

$$I_{bat} = \eta * \Delta V_f + \beta - I_{load} + I_{altss}$$
$$= \eta * \Delta V_f + \bar{\beta} \tag{4}$$

where $\bar{\beta} \triangleq \beta - I_{load} + I_{altss}$. Note that $\bar{\beta}$ is a constant if it is assumed that the changing load current, I_{load}, inducing the transient remains unchanged during the transient period. This is a reasonable assumption because a transient often lasts no more than 0.5 seconds. In addition, the parameter $\bar{\beta}$ is approximately equal to the change in load current that induced the transient, in the presence of a small battery charging or discharging current.

Therefore, equation (4) clearly characterizes the linear relationship between the two measured EPGS signals, I_{bat} and ΔV_f, which can be used to estimate the electric-current-generation efficiency of the alternator system, η.

2. Residual Generation

Based on the system model (4), a recursive-least-square (RLS) based parameter estimation method is employed for the generation of diagnosis residuals as detailed next.

Let us rewrite (4) as:

$$y(k) = \theta^T(k)u(k) \tag{5}$$

where $y(k)$ is the battery current (i.e., I_{bat}) at the k-th iteration, $\theta(k) \triangleq [\bar{\beta} \quad \eta]^T$, and $u(k) \triangleq [1 \quad \Delta V_f(k)]^T$. Now, based on the recursive-least-square algorithm [7]:

$$\begin{aligned} Q(k) &= \frac{P(k)u(k)}{\lambda + k(k)P(k)u(k)} \\ \hat{y}(k) &= \hat{\theta}^T(k)u(k) \\ \tilde{y}(k) &= y(k) - \hat{y}(k) \\ \hat{\theta}(k+1) &= \hat{\theta}(k) + Q(k)\tilde{y}(k) \\ P(k+1) &= \frac{1}{\lambda}\big(P(k) - Q(k)u^T(k)P(k)\big) \end{aligned} \tag{6}$$

where $\hat{\theta}(k) \triangleq \left[\hat{\bar{\beta}} \quad \hat{\eta}\right]^T$ is the estimated parameter vector, $\hat{\eta}$ and $\hat{\bar{\beta}}$ are the estimates for η and β, respectively, $\hat{y}$ is the estimated battery current, $\tilde{y}$ is the battery current estimation error, P is a 2×2 inverse correlation matrix, Q is a 2×1 gain vector, and λ is the exponential forgetting factor.

The estimated alternator current generation efficiency (i.e., $\hat{\eta}$) and the battery current estimation error (i.e., $\tilde{y}$) characterize the state of health of the alternator system. Thus, they can be used as diagnosis residuals for fault detection and isolation.

3. Residual Evaluation

In this subsection, the fault detection and isolation decision scheme employed in the residual evaluation process is detailed. As indicated earlier, two types of faults in the EPGS system are considered: belt slip and diode short. The relationship between the fault scenarios under consideration and the two diagnosis residuals is analyzed below.

- Under normal operating conditions, the estimate of the alternator-system current-generation-efficiency (i.e., $\hat{\eta}$) should remain high and positive, while the battery current estimation error (i.e., $\tilde{y}$) should be around zero.
- When belt slip occurs, the rotational speed of the alternator shaft drops, leading to a reduced alternator output current. As a result, the duty cycle of the field voltage is increased, i.e., $\Delta V_f > 0$. If the loss in alternator rotational speed is not significantly large, the alternator output current is able to increase and recover, i.e., $\Delta I_{alt} > 0$, but at the expense of a large increment in field voltage. Therefore, the estimated alternator-system current-generation-efficiency (i.e., $\hat{\eta}$) is low compared with its value under normal conditions. However, if the loss in alternator rotational speed is significantly large, the duty cycle of the field voltage reaches saturation, and the overall change in alternator current with respect to its steady-state value prior to the transient (i.e., I_{altss}) is negative, i.e., $\Delta I_{alt} < 0$. Therefore, the estimated alternator-system current-generation-efficiency (i.e., $\hat{\eta}$) is also negative and, hence, low.

- Finally, as a result of a diode short, one phase of the diode bridge rectifier in the alternator circuit always conducts current, and the alternator output current significantly oscillates. Consequently, the linear relationship between I_{bat} and ΔV_f, described by (4), is no longer satisfied, which is reflected on a significant battery current estimation error, i.e., $\tilde{y}$, defined in (6).

Based on the discussion above, the fault detection and isolation decision scheme is summarized in Table 1, where "H" and "L" represent high and low, respectively, and "x" represents that a diagnosis decision can be made without the corresponding residual.

Table 1: Fault detection and isolation decision scheme.

	Normal	Belt Slip	Shorted Diode
Estimated alternator system efficiency ($\hat{\eta}$)	H	L	X
Battery current estimation residual ($\lvert\tilde{y}\rvert$)	L	L	H

In more detail:

- If the estimated alternator system efficiency $\hat{\eta}$ is high and the battery current estimation residual $|\tilde{y}|$ is low, it is determined that no fault has occurred.
- If the estimated alternator system efficiency $\hat{\eta}$ is low and the battery current estimation residual $|\tilde{y}|$ is low, it is determined that belt slip has occurred.
- If the battery current estimation residual $|\tilde{y}|$ is high, it is determined that a diode short has occurred.

V. REAL-TIME ALGORITHM IMPLEMENTATION

The presented SOH monitoring method has been implemented using an automotive EPGS system test bench at General Motors R&D Center. In this section, the details of the real-time implementation of the SOH monitoring method are given.

1. EPGS System Test Bench

The EPGS system test bench is designed to emulate the behavior of practical EPGS systems, which provides a reliable platform for diagnostic data collection and algorithm validation. The test bench is composed of three major parts: the Dyno system, the automotive EPGS system, and the data acquisition and processing system. Figure 5 illustrates the schematic of the test bench, and Figure 6 shows a picture of the test bench.

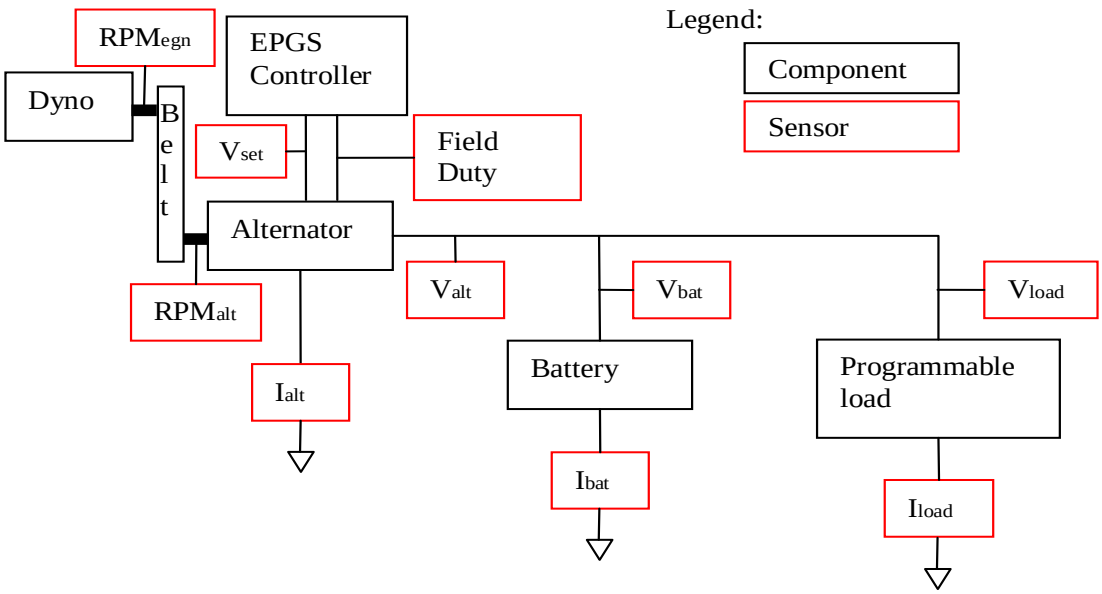

Figure 5: Schematic of EPGS system test bench.

The controlled dynamometer simulates the vehicle engine. Other components of the test bench include an alternator, a battery, a drive belt, a programmable electric load, a dSpace MicroAutoBox. The Dyno drives the alternator through the belt that connects the pulleys on the alternator and the Dyno shafts.

Belt slip is emulated by moving the alternator slightly towards the Dyno, so the tension of the drive belt is relaxed. Diode short is emulated by connecting a high-power, low-resistance resistor in parallel to one of the diode rectifiers in the alternator.

The sensor measurements of current, voltage, and speed are fed to the dSpace MicroAutoBox module in which the diagnosis and control software can be uploaded for execution in real time. The MicroAutoBox module also allows data monitoring and logging through a link to a laptop computer. The sensor measurements are also fed to a bank of Fluke Precision Multimeters and to a high-end Yokogawa oscilloscope, which can also record the data for analysis off-line.

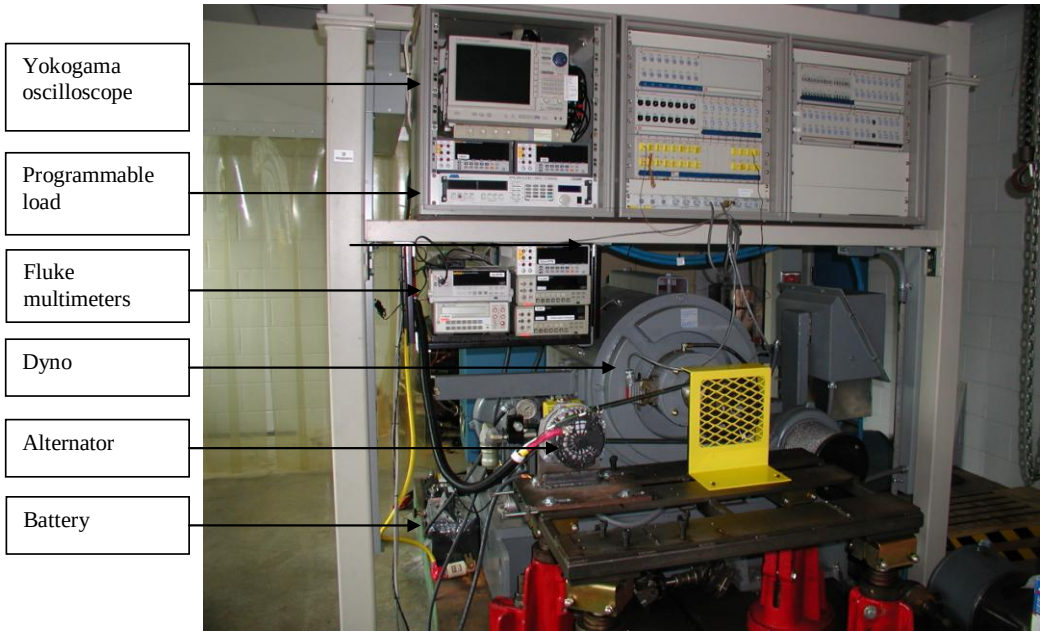

Figure 6: EPGS system test bench.

2. Real-Time Implementation of SOH Monitoring Algorithm

Figure 7 is a block diagram illustrating the operations involved in the real-time implementation of the SOH monitoring method.

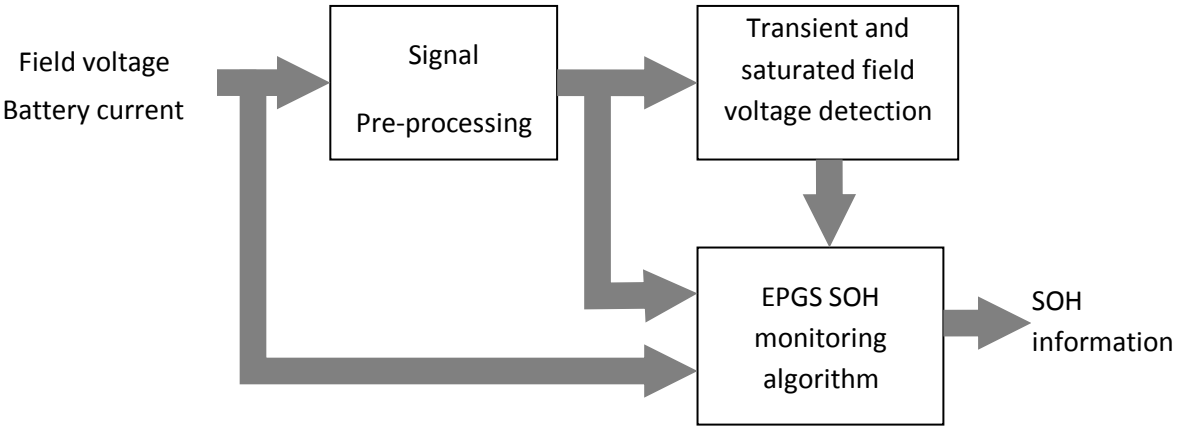

Figure 7: Block diagram of the implementation of the real-time SOH monitoring method.

As can be seen, the duty cycle of the field voltage, V_f, which from now on will be referred as "field voltage" for simplicity, and the battery current, I_{bat}, signals go through a preprocessing component to remove noise and to generate useful features. These features are then used to detect the beginning, end, and type of transients (caused by changes in the vehicle's electrical load), as well as to determine whether the field voltage is saturated. Finally, this information along with the raw and preprocessed signals is used by the SOH monitoring algorithm to generate diagnostic residuals, including the alternator-system efficiency estimate (i.e., $\hat{\eta}$) and the alternator current estimation error (i.e., $\tilde{y}$). The residuals are used to determine the SOH status by following the FDI decision scheme described in Section IV. Notice that the SOH monitoring algorithm is fed with both raw data and pre-processed data. The raw data is used for the generation of

the diagnosis residuals during transient operation while, in addition, the pre-processed data is used for the generation of the diagnosis residuals during steady-state operation because, as will be shown, the raw EPGS signals (e.g., the field voltage and battery current) are noisy even at steady state, which could result in inaccuracy of the diagnosis residuals.

The implementation of each component shown in Figure 7 is described next.

A. Signal Pre-Processing

The EPGS system signals present significant variations, or noise, especially under diode short condition, which make the fault diagnosis and parameter estimation tasks much more difficult. The main objective of the signal pre-processing component is to prepare the EPGS system signals for detecting the transients caused by changes in the vehicle's electrical load.

A straightforward method for transient detection is based on measuring the instantaneous change in the battery current and/or field voltage. However, in the presence of the diode short fault, there are always significant oscillations in the signals (as shown in Figure 8). Therefore, the instantaneous change in the EPGS signals cannot be used as a robust feature for transient detection, as can be seen in Figure 9. Hence, it is necessary to pre-process the raw signal samples to obtain useful information. In this project, certain filtering techniques are used to reduce the effect of significant noise oscillations during steady-state operation and as a result of diode short fault.

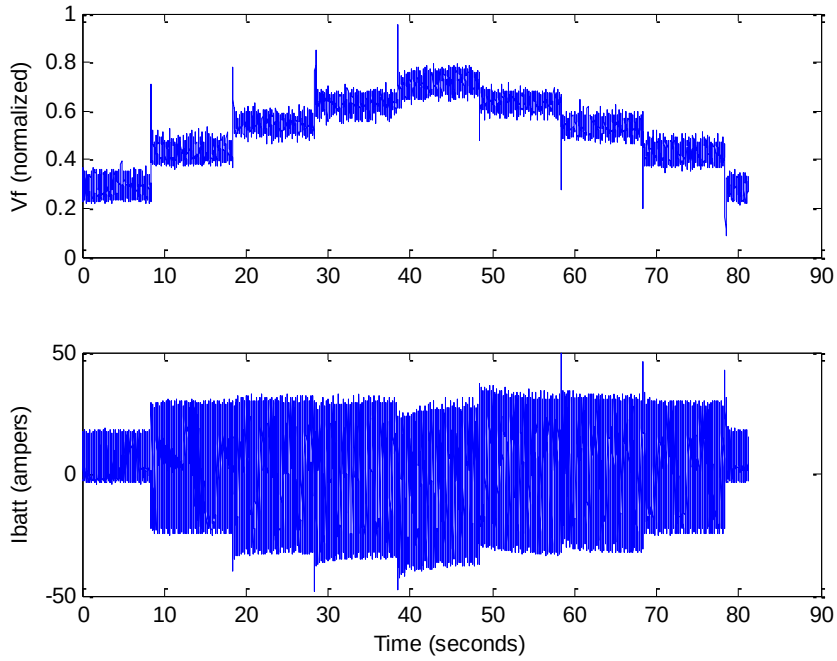

Figure 8: Field voltage and battery current under diode short condition.

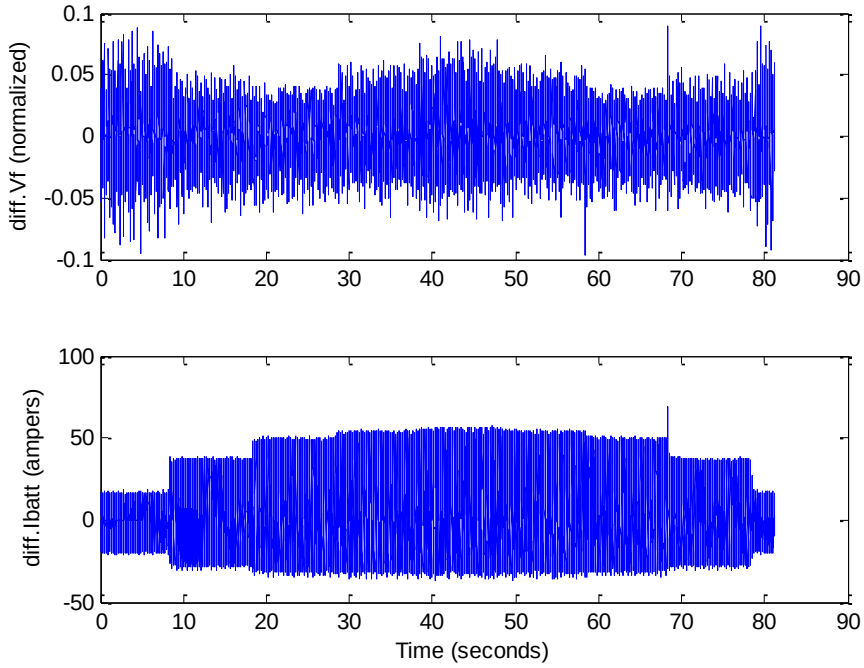

Figure 9: Instantaneous change in field voltage and battery current under diode short condition.

Initially, the signals are filtered by computing their simple averages over of 20 samples: average field voltage, V_{f_avg}, and average battery current, I_{bat_avg}. In the EPGS system test bench, the sampling rate is 10 kHz. For the sake of computational efficiency, the SOH monitoring method is carried out at a low sampling rate. Specifically, the raw signals are downsampled to 400 Hz. Therefore, each of these averages is computed over a fixed time-window of 50 milliseconds. However, even after averaging, these signals still present significant variations that can generate false transient detections. Nonetheless, these averages are still needed for the detection of the end of a transient (subsection B) and the generation of the diagnosis residuals during-steady operation (subsection C).

In view of this, for better filtering, moving averages are computed. For instance, a moving average of the battery current, $\bar{I}_{bat}$, is computed as:

$$\bar{I}_{bat}(k) = \frac{1}{N_1} \sum_{i=k-N_1+1}^{k} I_{bat}(k) \tag{7}$$

where N_1 is the number of samples. More exactly, N_1 is set to 60 for the computation of the moving average of the battery current, $\bar{I}_{bat}$, and to 40 for the computation of the moving average of the field voltage, $\bar{V}_f$. A larger number samples for the computation of moving average of the battery current is needed because this signal contains the most noise and oscillations in the presence of a diode short fault.

Figure 10 shows the moving averages of the field voltage and battery current. As can be seen, the signals present a lot less noise compared to the raw signals in Figure 8, and the transients due to change in electrical load are clearly defined by near vertical slopes.

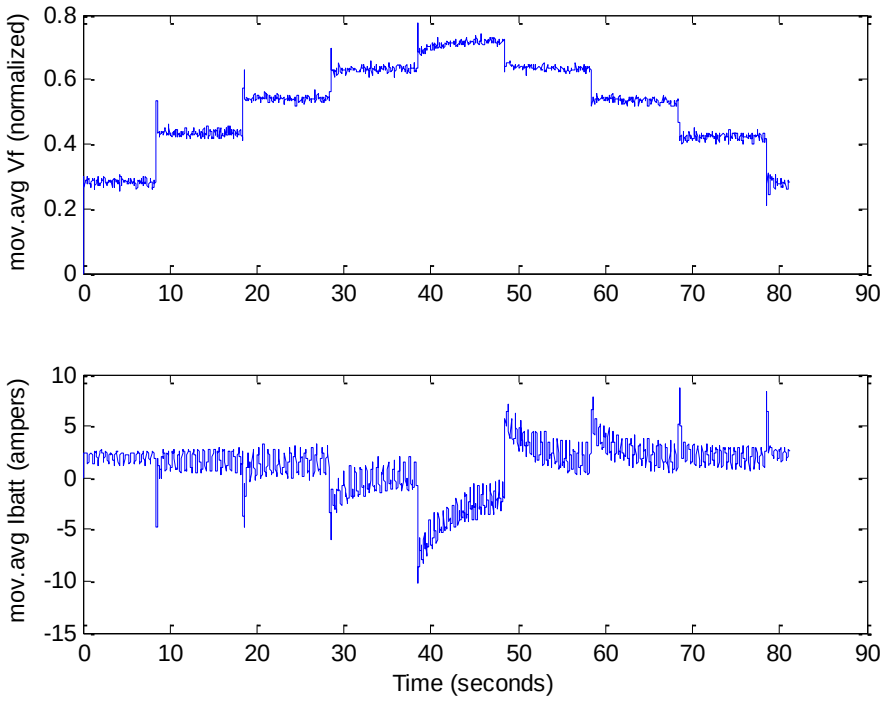

Figure 10: Moving averages of the field voltage and battery current under diode short condition.

In order to detect transients, a second set of moving averages of the field voltage and battery current, $\bar{\bar{V}}_f$ and $\bar{\bar{I}}_{bat}$ respectively, is also needed. Specifically, the second moving average of the battery current is computed as:

$$\bar{\bar{I}}_{bat}(k) = \frac{1}{N_2} \sum_{i=k-N_2+1}^{k} I_{bat}(k - N_1) \tag{8}$$

where N_2 is the window size, and k denotes the current sample. As can be seen, the raw battery current is delayed by N_1 samples in the computation of the second moving average. Therefore, at any sampling period k, the first and second moving averages, $\bar{I}_{bat}$ and $\bar{\bar{I}}_{bat}$, are independent. The number of samples used in the computation of this second

set of moving averages N_2 is larger than in the first set: 80 samples from the field voltage, and 120 samples from the battery current.

Finally, useful features that characterize the occurrence of transient periods resulting from changes in electrical load are constructed for the field voltage and battery current. Specifically, they are:

$$\underline{\Delta} I_{bat}(k) = \bar{I}_{bat}(k) - \bar{\bar{I}}_{bat}(k)\,,$$
$$\underline{\Delta} V_f(k) = \bar{V}_f(k) - \bar{\bar{V}}_f(k)\,. \tag{9}$$

The extracted features $\underline{\Delta} I_{bat}$ and $\underline{\Delta} V_f$ are shown in Figure 11.

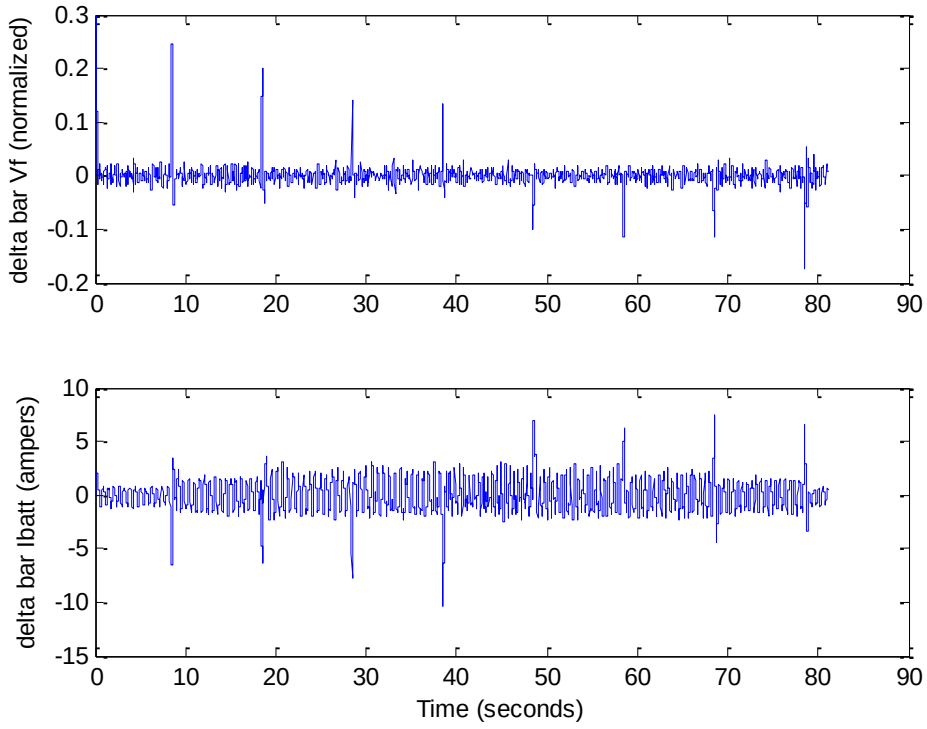

Figure 11: Extracted features in field voltage and battery current under diode short condition after pre-processing.

As can be seen, the heavy noise and oscillations seen in the instantaneous change in the raw field voltage and battery current signals (see Figure 9) have been suppressed, and the effect of changes in the vehicle's electrical load are clearly seen as sharp peaks. Therefore, the transient periods can be successfully detected by using the extracted features $\underline{\Delta}I_{bat}$ and $\underline{\Delta}V_f$.

B. Transient and Saturated Filed Voltage Detection

In the real-time implementation of the SOH monitoring method, the start of a transient due to a change in electrical load is detected by combining the features in field voltage and battery current, namely, $\underline{\Delta}V_f$ and $\underline{\Delta}I_{bat}$, that were derived in Section A, into a single feature $d(k)$:

$$d(k) = r\underline{\Delta}V_f(k) - \underline{\Delta}I_{bat}(k) \tag{10}$$

where r is a scaling coefficient to normalize $\underline{\Delta}V_f$ since this is very small, from 0 to a theoretical maximum of 1, compared with $\underline{\Delta}I_{bat}$, which can reach several amperes. In this project, the scaling factor *r* was set equal to 50.

In the next page, Figure 12 shows the plot of the transient detection feature $d(k)$ under diode short condition. A large positive peak indicates an increment in electric load, and a large negative peak indicates a reduction in electrical load. Therefore, upper and lower thresholds can be set to detect the beginning of a transient, as well as to identify the direction of the change in electrical load. In this project, the upper and lower thresholds were set equal to 8 and -8, respectively.

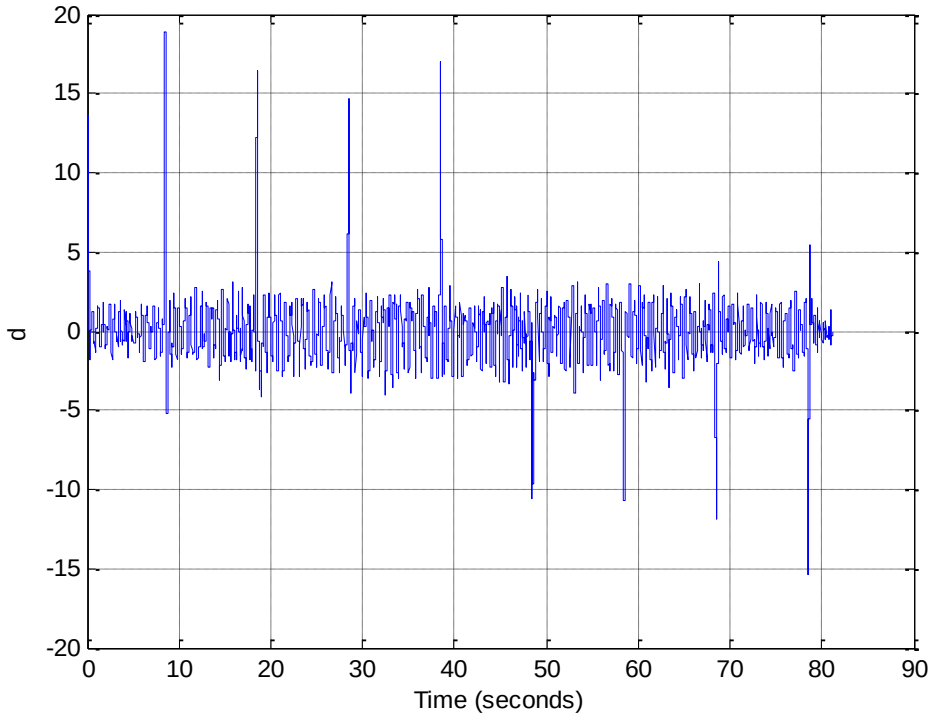

Figure 12: Transient detection feature under diode short condition

The detection of the end of a transient is more straightforward. A transient has ended when the simple average of the battery current, I_{bat_avg}, which was described in subsection A, has reached steady state, i.e., when its instantaneous change is small.

Before generating the diagnosis residuals, i.e., $\hat{\eta}$ and $|\tilde{y}|$, it is also necessary to know whether the field voltage is saturated. This is accomplished by checking if the absolute value of the $\underline{\Delta}V_f$ feature, in (9), which describes the change in field voltage, is small, i.e., $\left|\underline{\Delta}V_f(k)\right| < \delta$, where δ is an small quantity, which in this project was set equal to 0.05. Notice that the saturated field voltage condition is only checked when a change in load current has been detected, that is, at the beginning of the transient, but not thereafter. Additionally, the saturation of filed voltage duty cycle can also be detected by checking if it is close to 1.

C. Residual Generation and Evaluation

The SOH monitoring algorithm, including residual generation and evaluation, has been described in Section IV. The alternator system efficiency and battery current estimation error are generated based on (4) and (6). Then, the fault detection and isolation decision scheme given in Table 1 is employed to determine the SOH status of the alternator system.

Notice that during steady-state operation, there is not enough excitation in the EPGS system signals. Hence, it is not suitable to apply the recursive-least-square algorithm. Thus, during steady-state operation, the efficiency of the alternator system is approximated by the ratio between the change in battery current $\Delta \mathrm{I}_{bat}$ and the change in field voltage $\Delta \mathrm{V}_f$ after a change in the electrical load occurs, that is:

$$\eta = \frac{\Delta \mathrm{I_{alt}}}{\Delta \mathrm{V_f}} \cong \frac{\Delta \mathrm{I_{bat}}}{\Delta \mathrm{V_f}} \ . \tag{11}$$

Specifically, during steady-state operation, the change in battery current (i.e., $\Delta \mathrm{I}_{bat}$) is computed as the difference between the present average battery current I_{bat_avg} with respect to a reference battery current value (i.e., I_{bat0}), which is defined as the minimum battery current value during the transient due to an increment in electrical load or as the maximum battery current value during the transient due to a decrement in electrical load. Similarly, the change in field voltage (i.e., $\Delta \mathrm{V}_f$) is computed as the difference between the present average field voltage V_{f_avg} with respect to a reference field voltage value (i.e., V_{f0}), which is defined as the minimum field voltage value during the transient due to an increment in electrical load or as the maximum field voltage value during the

transient due to a decrement in electrical load. To summarize, the efficiency of the alternator system is estimated as:

$$\hat{\eta} = \frac{\Delta \mathrm{I}_{bat}}{\Delta \mathrm{V}_f} = \frac{\mathrm{I}_{bat\_avg} - \mathrm{I}_{bat0}}{\mathrm{V}_{f\_avg} - \mathrm{V}_{f0}} \ . \tag{12}$$

Care must be taken if the field voltage is already saturated. In this case, $\Delta \mathrm{V}_f$ would become zero since the field voltage is no longer changing. Therefore, when a change in electrical load is detected, the reference field voltage V_{f0} is not updated, i.e., it retains its previous value. In addition, when computing $\Delta \mathrm{I}_{bat}$ using (12), the change in load current, $\Delta \mathrm{I}_{load}$, estimated from the battery-current transient, must be taken into account. For instance, if the load current was increased by $\Delta \mathrm{I}_{load}$ when the field voltage is saturated, then $\Delta \mathrm{I}_{load}$ should be subtracted from I_{bat0} in order to obtain an accurate estimate of $\Delta \mathrm{I}_{bat}$ corresponding to the amount $\Delta \mathrm{V}_f$ under consideration. Recall that battery current signal, I_{bat}, is negative when the battery is sourcing current, i.e., discharging.

Complementarily, during steady-state operation, the battery current estimation error, $\tilde{y}$, is approximated by the difference between the raw battery current signal, I_{bat}, and the average of the battery current signal, I_{bat_avg}, that is:

$$\hat{\tilde{y}} \ = \ \mathrm{I}_{bat} - \mathrm{I}_{bat\_avg} \tag{13}$$

whose magnitude is proportional to the amount of noise in the battery current signal and, under constant electrical load condition, is also proportional to the amount of noise in the alternator output current, which, as was explained in Section III, is very large when there is a diode short fault.

During the residual evaluation procedure, thresholds should be chosen for the estimated alternator-system efficiency and battery current estimation error. In the real-time implementation, the thresholds for the estimated alternator-system efficiency (i.e., $\hat{\eta}$) and battery current estimation residual (i.e., $|\tilde{y}|$) were chosen to be 0 and 7, respectively.

3. dSpace/Simulink System for Real-time SOH Monitoring

Figure 13 shows the implementation of the real-time state of health (SOH) monitoring method in Simulink. As can be seen to the left, the input signals are the field voltage (V_f), the battery current (I_{bat}), and the engine speed (E_{ngRPM}). The "Counter Limited" signal generator is used for downsampling of the input signals. The outputs, BeltSlip and DiodeShort, are the diagnosis results in binary form, which indicate if the diagnosis residuals have exceed their corresponding fault detection thresholds.

Figure 14 shows how the diagnosis results are generated inside the "Fault Detection & Isolation" subsystem in Figure 13. The engine speed signal (E_{ngRPM}) is solely used to enable the algorithm when the engine speed is within a given range, more exactly, for the example in Figure 14, when the engine speed is between 750 and 2050 RPM. The alternator system efficiency (i.e., $\hat{\eta}$) and battery current estimation error (i.e., $\tilde{y}$) are generated by the "Estimation" subsystem. Then, the diagnosis residuals go through low-pass filters to finally be compared with their corresponding fault detection thresholds. In addition, notice that the battery current estimation error is passed through and absolute-value block to convert it in a unsigned quantity (i.e., $|\tilde{y}|$) or residual that can be easily evaluated.

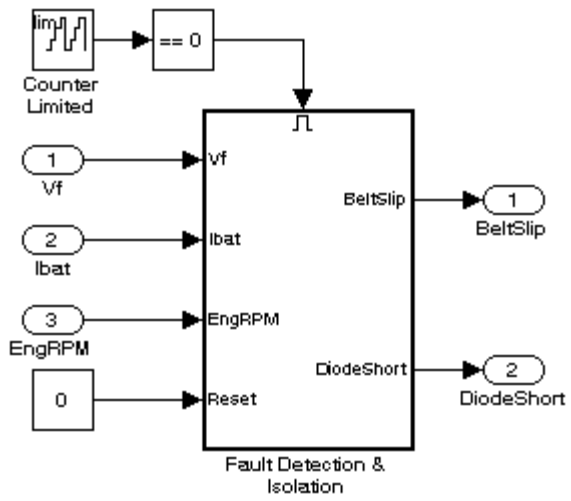

Figure 13: Real-time SOH monitoring method in Simulink.

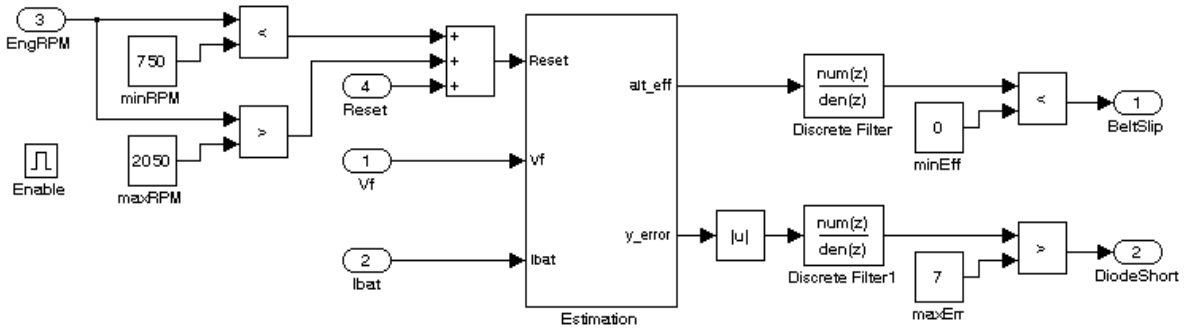

Figure 14: Fault detection and isolation subsystem.

Figure 15 shows the implementation of the "Estimation" subsystem. Here, the "Operating Condition Identification & Estimation" block is an Embedded Matlab Block which contains the real-time algorithm that generates the estimations of the diagnosis parameters as was described in the previous subsections and Section IV.

The Simulink implementation of the real-time SHO monitoring method was converted in an embedded software program and uploaded to the dSpace MicroAutoBox

module of the EPGS system test bench at GM R&D Center for testing on-line. Figure 16 shows a graphical user interface in ControlDesk used for the control of the test bench and monitoring/logging of the EPGS system signals, and diagnosis residuals/results.

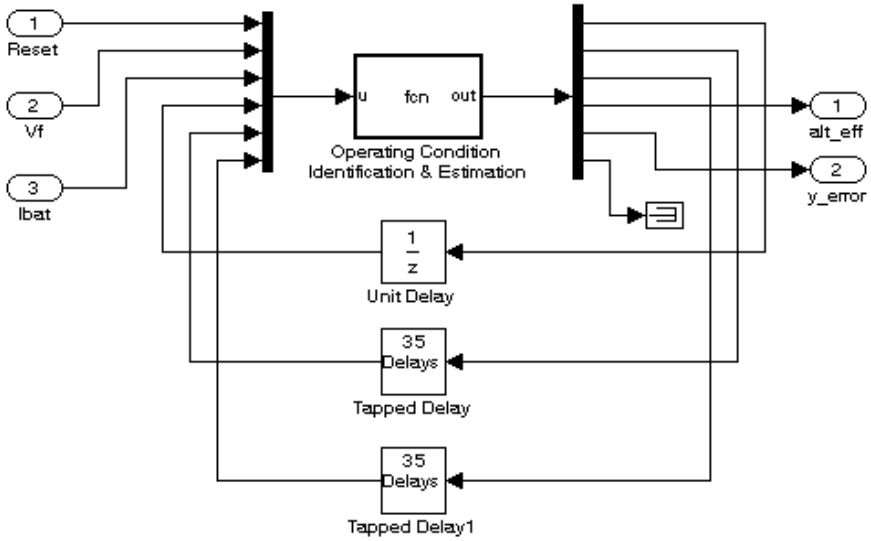

Figure 15: Alternator system efficiency and battery current estimation error generator.

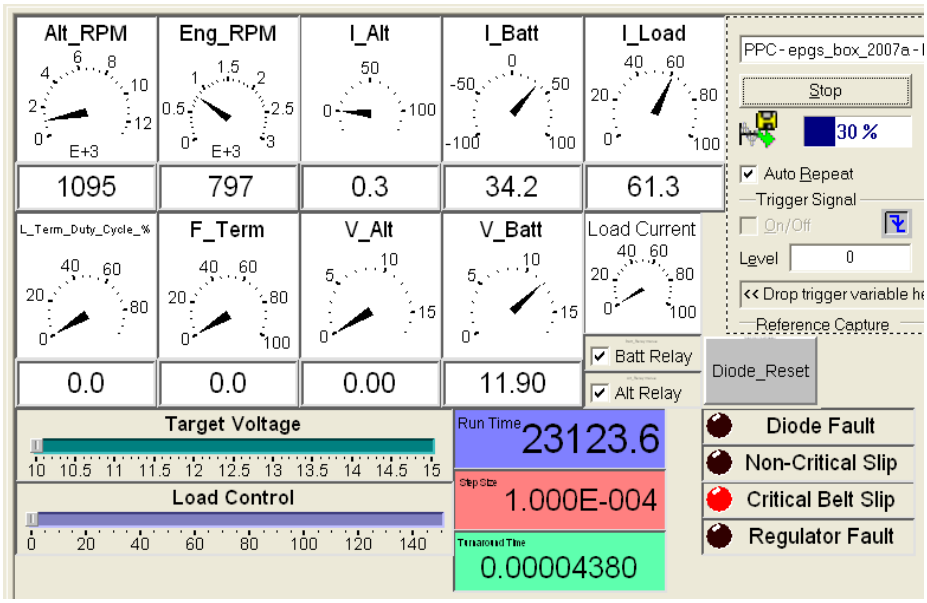

Figure 16: ControlDesk graphical user interface for real-time SOH monitoring.

VI. ALGORITHM PERFORMANCE EVALUATION RESULTS

The SOH monitoring method has been validated at various operating conditions using the EPGS system test bench at GM R&D Center. In this section, several representative case studies to illustrate the effectiveness and robustness of the fault diagnosis algorithm are shown. Specifically, three major cases are presented: low engine speed, high engine speed, and time-variant engine speed.

1. Evaluation Results at Low Engine Speed Condition

The validation results corresponding to the case of low engine speed (specifically, 800 RPM) are reported in Figure 17 to Figure 22.

For the case of normal operating condition, the EPGS system signals are shown in Figure 17, and the alternator system efficiency estimate $\hat{\eta}$ and battery current estimation residual $|\tilde{y}|$ are given in Figure 18. As we can see, $\hat{\eta}$ remains high (compared with a threshold of 0), and $|\tilde{y}|$ remains low (compared with a threshold of 7). Therefore, based on the fault detection and isolation decision scheme described in Section IV, we can conclude that the system is "healthy".

The case of belt slip is reported in Figure 19 and Figure 20. The EPGS system signals are given in Figure 19, and the diagnostic residuals are shown in Figure 20. As can be seen from Figure 20, as the alternator-to-engine RPM ratio drops from approximately 3 to 2 as a result of belt slip, the alternator system efficiency estimate $\hat{\eta}$

also decreases significantly and reaches negative values. In addition, the battery current estimation residual $|\tilde{y}|$ remains low. Therefore, based on the fault detection and isolation decision scheme described in Section IV, we can conclude the occurrence of a belt slip fault.

The case of shorted diode is reported in Figure 21 and Figure 22. Specifically, Figure 21 shows the EPGS system signals, and Figure 22 gives the corresponding diagnostic residuals. As shown in Figure 22, the battery current estimation residual $|\tilde{y}|$ is much higher (compared with a threshold of 7) than the one at "healthy" condition (shown in Figure 18), indicating the occurrence of a diode short fault. Moreover, it is worth noting that when there is no electric load, this residual remains low.

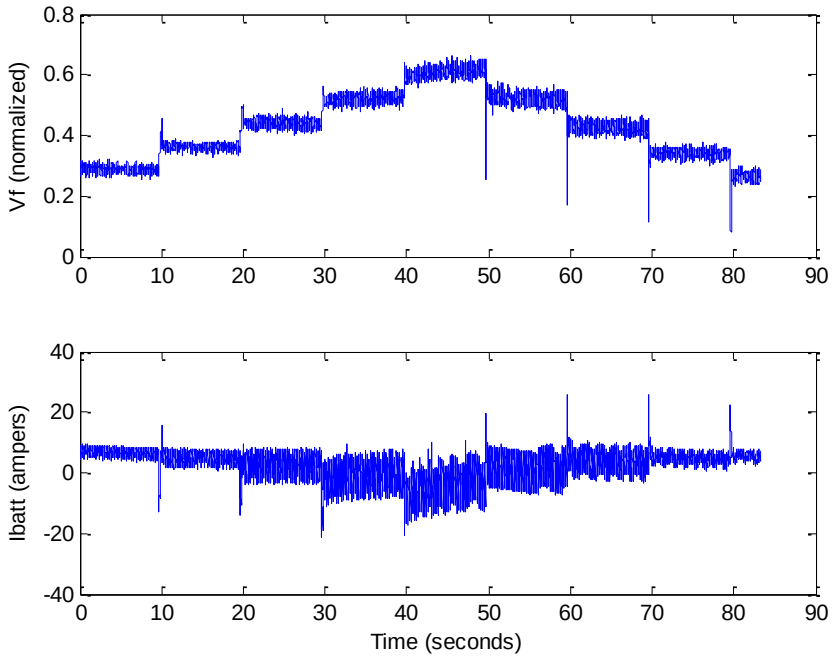

Figure 17: Field voltage and battery current under normal condition at 800 engine RPM.

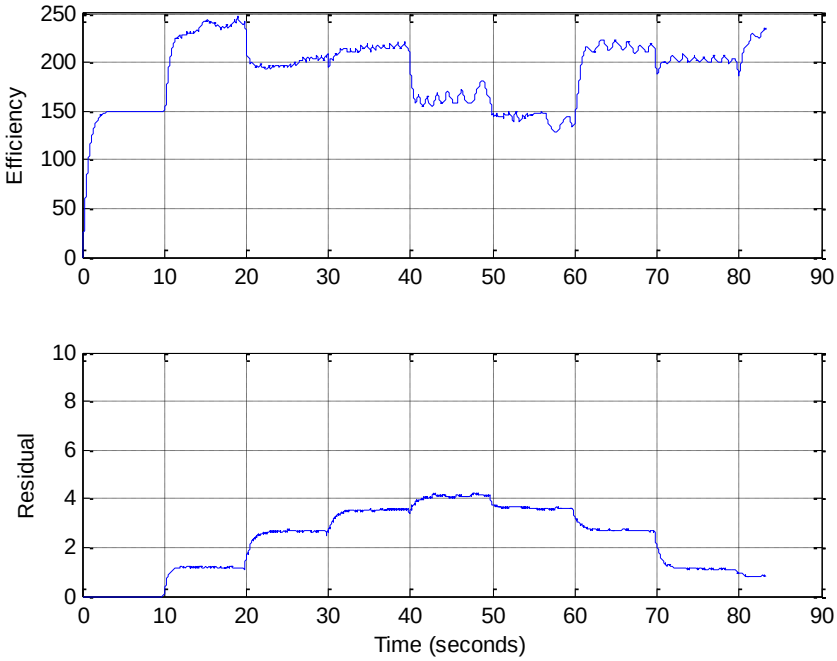

Figure 18: Alternator system efficiency and battery current estimation residual under normal condition at 800 engine RPM.

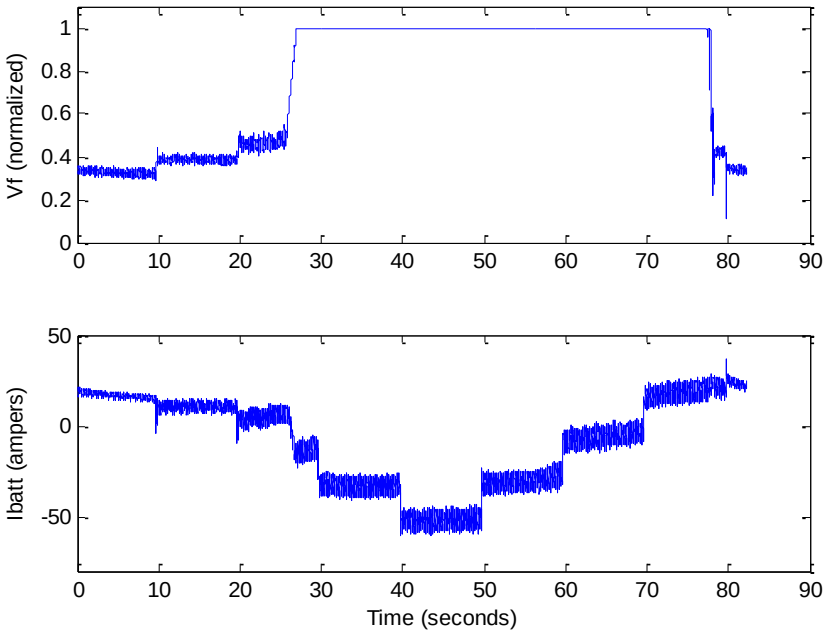

Figure 19: Field voltage and battery current under belt slip condition at 800 engine RPM.

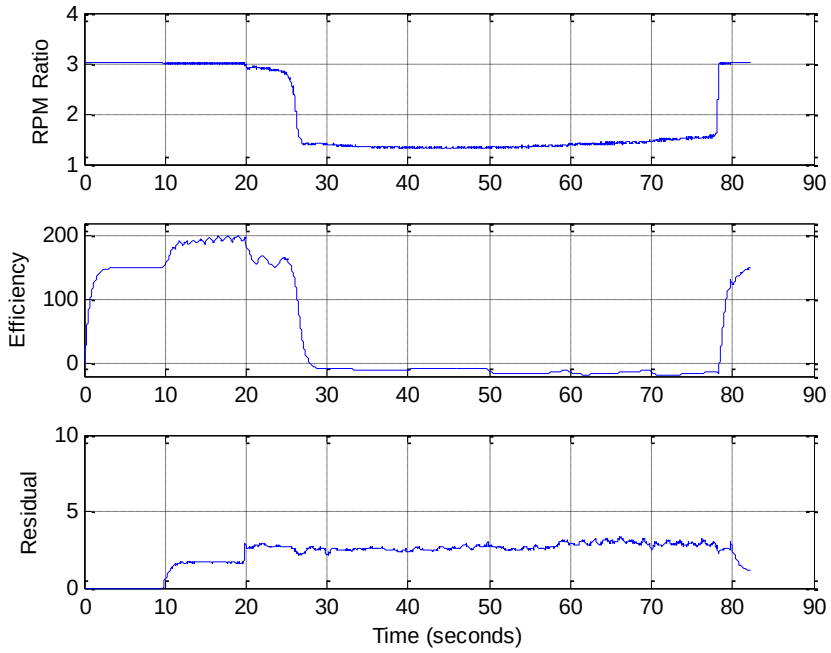

Figure 20: Alternator-to-engine RPM ratio, alternator system efficiency, and battery current estimation residual under belt slip condition at 800 engine RPM.

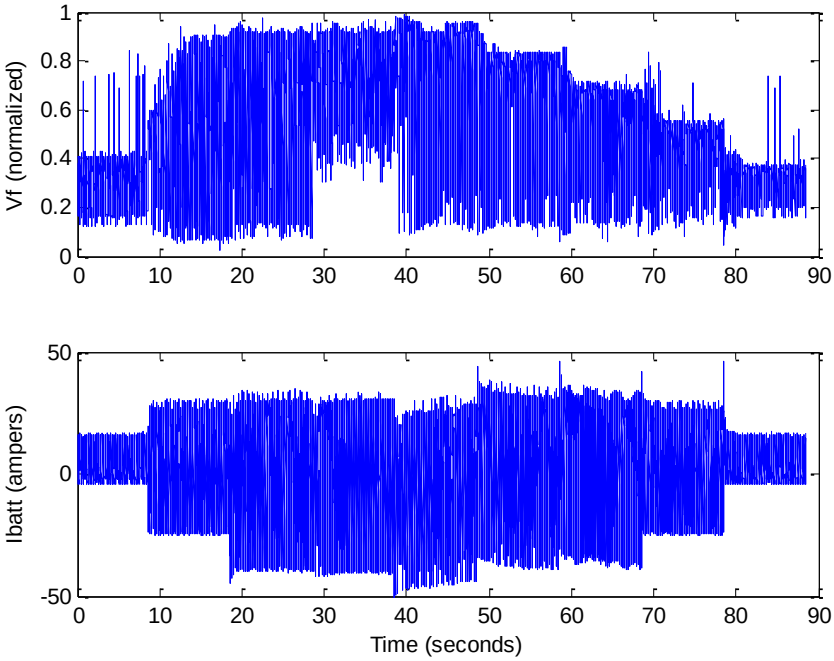

Figure 21: Field voltage and battery current under diode short condition at 800 engine RPM.

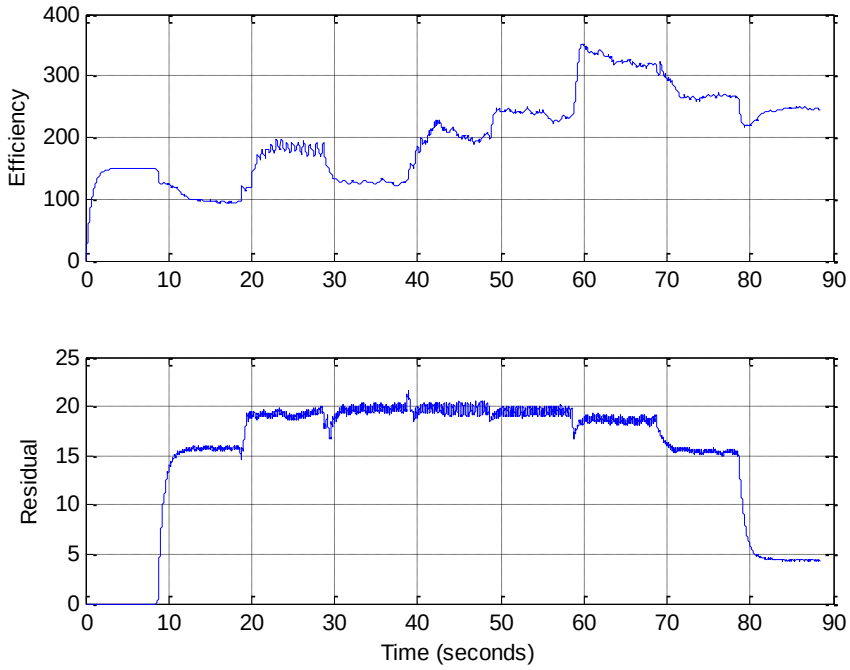

Figure 22: Alternator system efficiency and battery current estimation residual under diode short condition at 800 engine RPM.

2. Evaluation Results at High Engine Speed Condition

Figure 23 to Figure 28 show the EPGS system signals, the alternator system efficiency, and the battery current estimation residual under normal, belt slip, and diode short conditions at high engine speeds, mostly, 2000 RPM, except in the case of belt slip, in which case the engine speed is only 1000 RPM because it is difficult to induce this type of fault at higher speeds.

For the case of normal operating condition, the EPGS system signals are shown in Figure 23, and the alternator system efficiency estimate $\hat{\eta}$ and battery current estimation residual $|\tilde{y}|$ are given in Figure 24. As we can see, $\hat{\eta}$ remains high (compared with a threshold of 0), and $|\tilde{y}|$ remains low (compared with a threshold of 7). Therefore, based

on the fault detection and isolation decision scheme described in Section IV, we can conclude that the system is "healthy".

For the case of belt slip, the EPGS system signals are given in Figure 25, and the diagnostic residuals are shown in Figure 26. As can be seen from Figure 26, as the alternator-to-engine RPM ratio drops from approximately 3 to 2 as a result of belt slip, the alternator system efficiency estimate $\hat{\eta}$ also decreases significantly and reaches negative values. In addition, the battery current estimation residual $|\tilde{y}|$ remains low. Therefore, based on the fault detection and isolation decision scheme described in Section IV, we can conclude the occurrence of a belt slip fault.

The case of shorted diode is reported in Figure 27 and Figure 28. Specifically, Figure 27 shows the EPGS system signals, and Figure 28 gives the corresponding diagnostic residuals. As shown in Figure 28, the battery current estimation residual $|\tilde{y}|$ is much higher (compared with a threshold of 7) than the one at "healthy" condition (shown in Figure 24), indicating the occurrence of a diode short fault. Moreover, it is worth noting that when there is no electric load, this residual remains low.

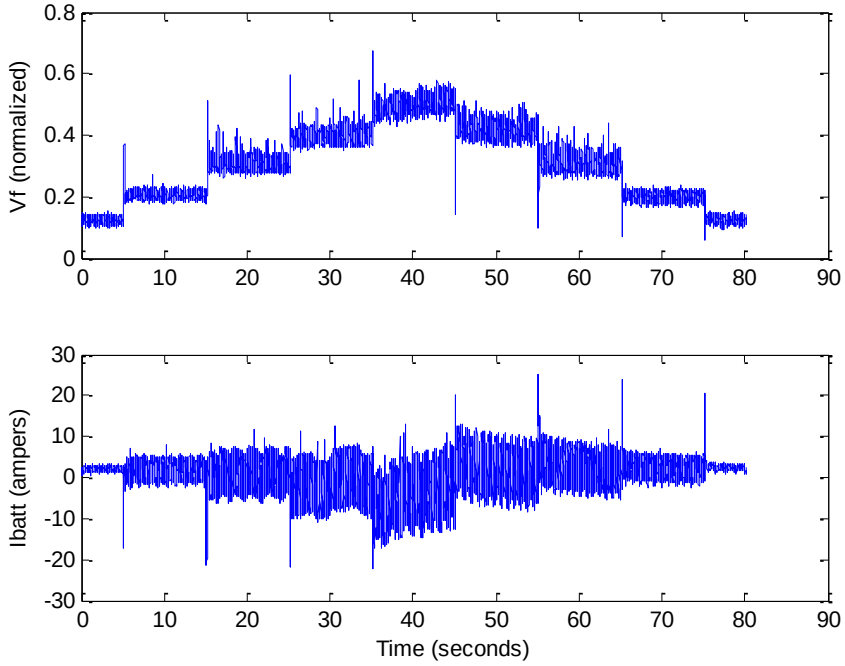

Figure 23: Field voltage and battery current under normal condition at 2000 engine RPM.

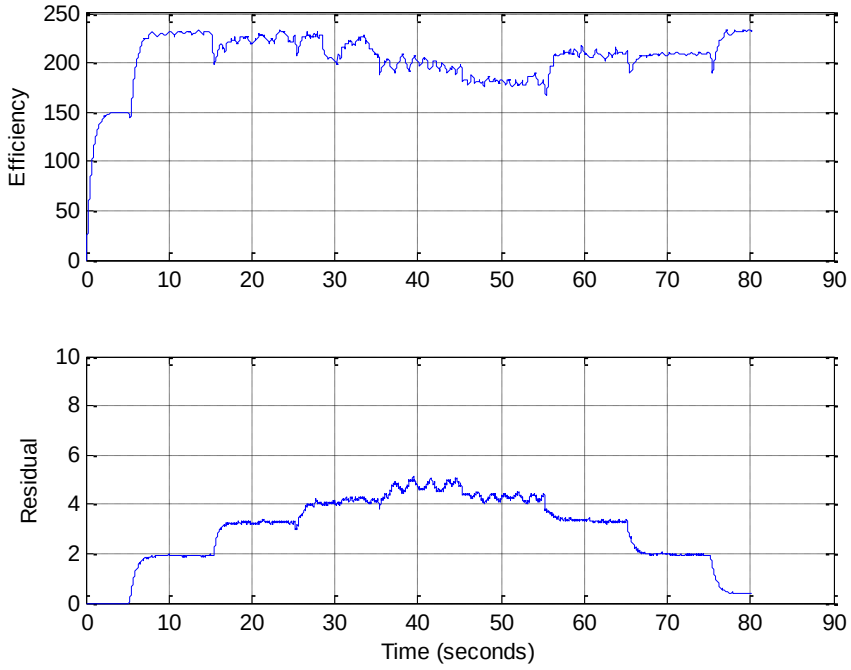

Figure 24: Alternator system efficiency and battery current estimation residual under normal condition at 2000 engine RPM.

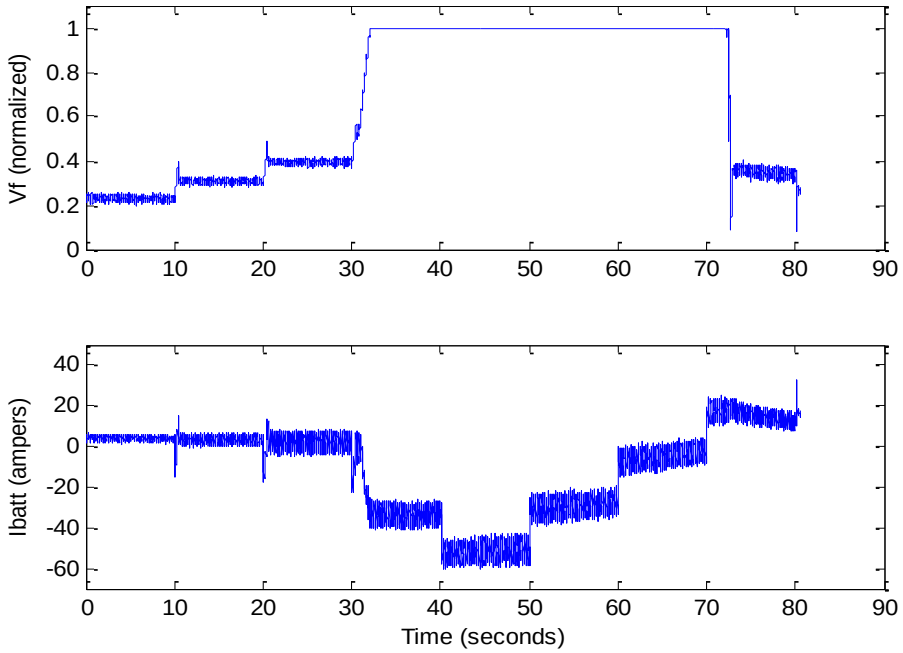

Figure 25: Field voltage and battery current under belt slip condition at 1000 engine RPM.

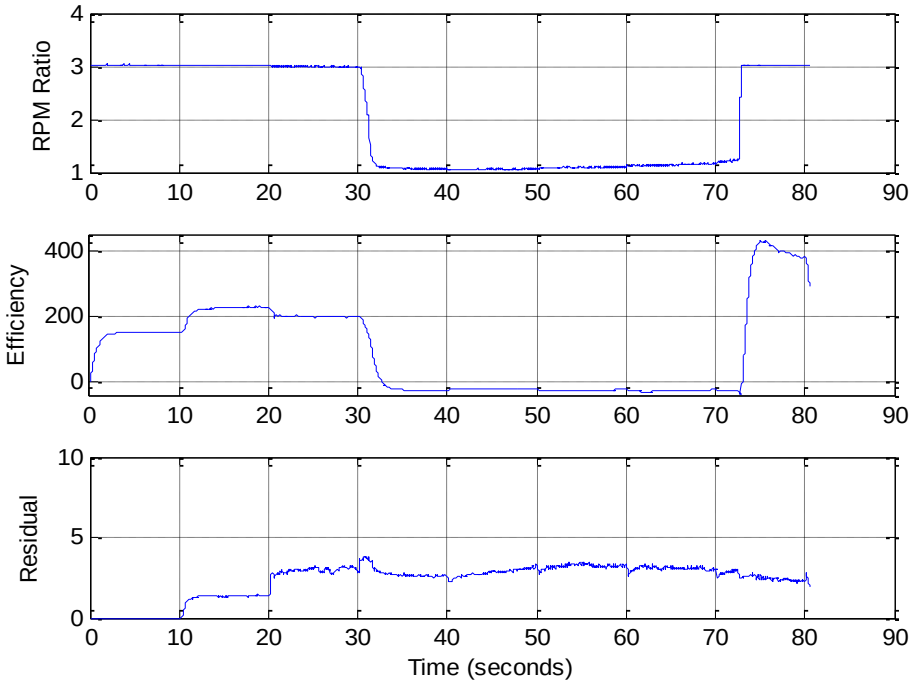

Figure 26: Alternator-to-engine RPM ratio, alternator system efficiency, and battery current estimation residual under belt slip condition at 1000 engine RPM.

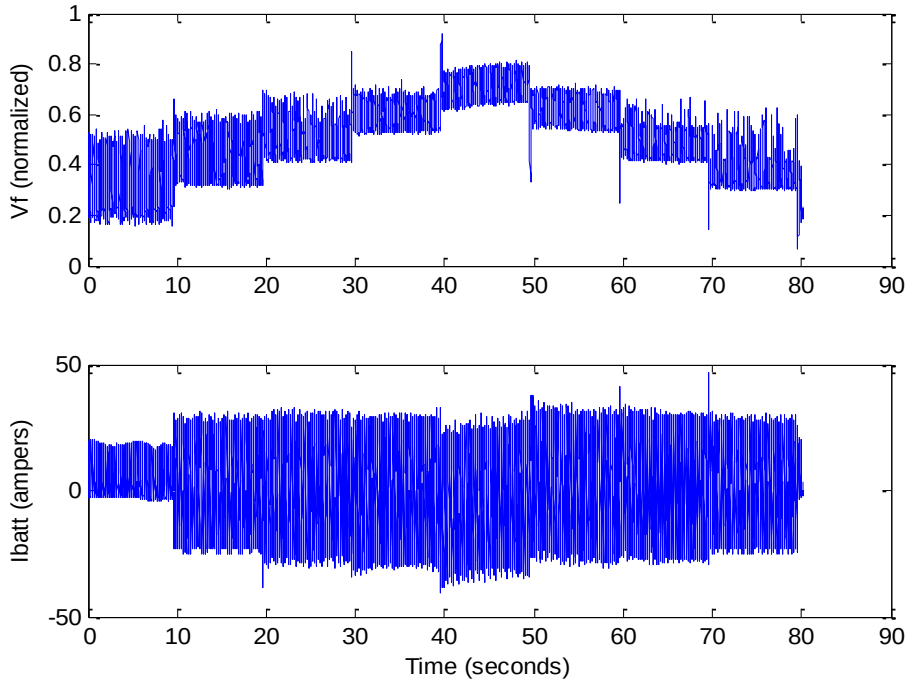

Figure 27: Field voltage and battery current under diode short condition at 2000 engine RPM.

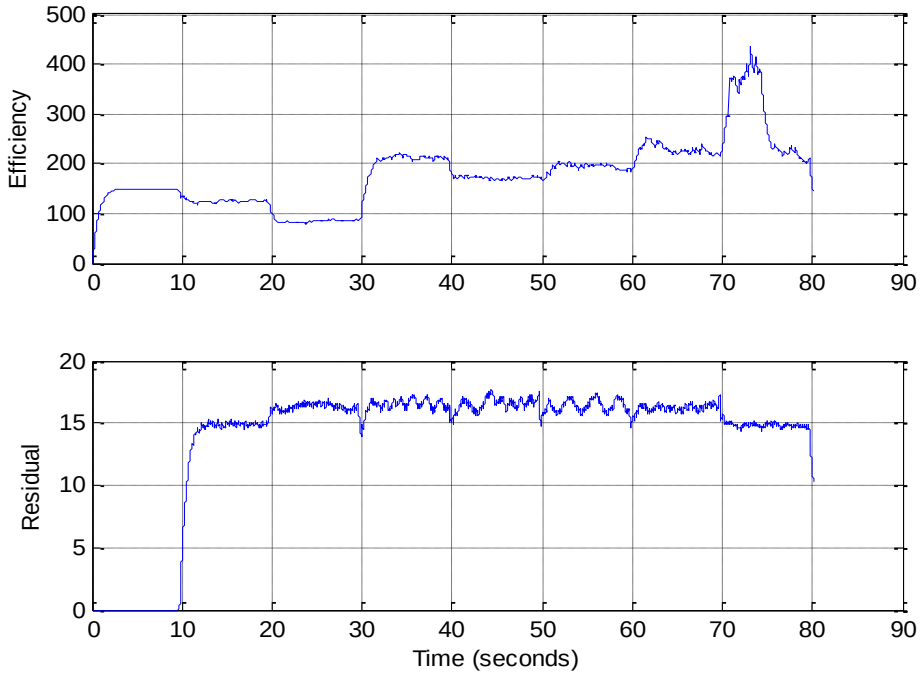

Figure 28: Alternator system efficiency and battery current estimation residual under diode short condition at 2000 engine RPM.

3. Evaluation Results at Time-Varying Engine Speed Condition

Figure 29 to Figure 34 show the EPGS system signals, the estimated alternator system efficiency, and the battery current estimation residual under normal, belt slip, and diode short conditions and time-varying engine speeds.

For the case of normal operating condition, the EPGS system signals are shown in Figure 29, and the alternator system efficiency estimate $\hat{\eta}$ and battery current estimation residual $|\tilde{y}|$ are given in Figure 30. As we can see, $\hat{\eta}$ remains high (compared with a threshold of 0), and $|\tilde{y}|$ remain low (compared with a threshold of 7). Therefore, based on the fault detection and isolation decision scheme described in Section IV, we can conclude that the system is "healthy".

For the case of belt slip, the EPGS system signals are given in Figure 31, and the diagnostic residuals are shown in Figure 32. As can be seen from Figure 32, as the alternator-to-engine RPM ratio drops from approximately 3 to 2, as a result of belt slip, the alternator system efficiency estimate $\hat{\eta}$ also decreases significantly and reaches negative values. In addition, the battery current estimation residual $|\tilde{y}|$ remains low. Therefore, based on the fault detection and isolation decision scheme described in Section IV, we can conclude the occurrence of a belt slip fault.

The case of shorted diode is reported in Figure 33 and Figure 34. Specifically, Figure 33 shows the EPGS system signals, and Figure 34 gives the corresponding diagnostic residuals. As shown in Figure 34 the battery current estimation residual $|\tilde{y}|$ is much higher (compared with a threshold of 7) than the one at "healthy" condition (shown in Figure 30), indicating the occurrence of a diode short fault. Moreover, it is worth noting that when there is no electric load, this residual remains low.

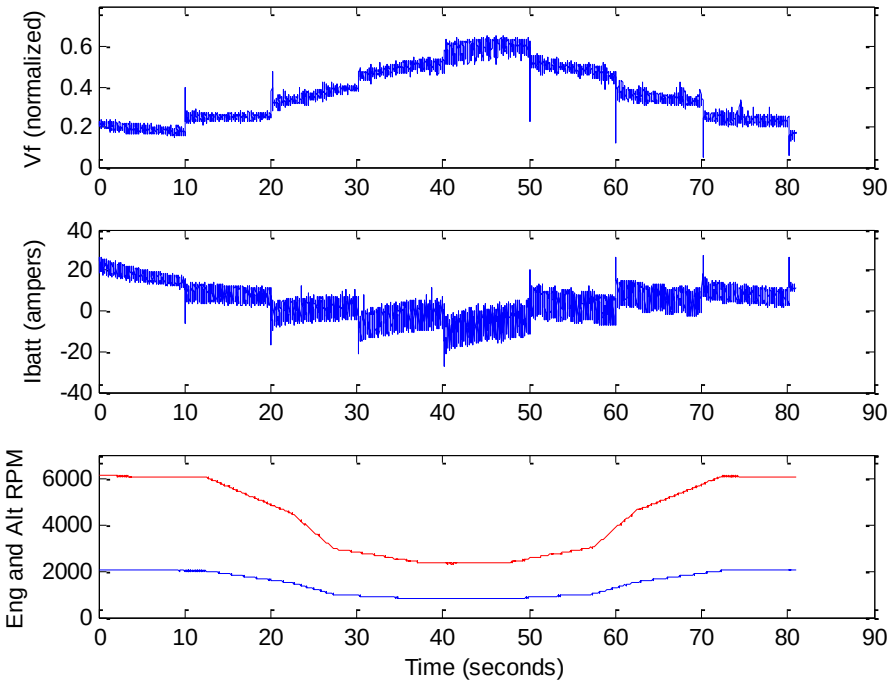

Figure 29: Field voltage, battery current, and alternator RPM vs. varying engine RPM under normal condition.

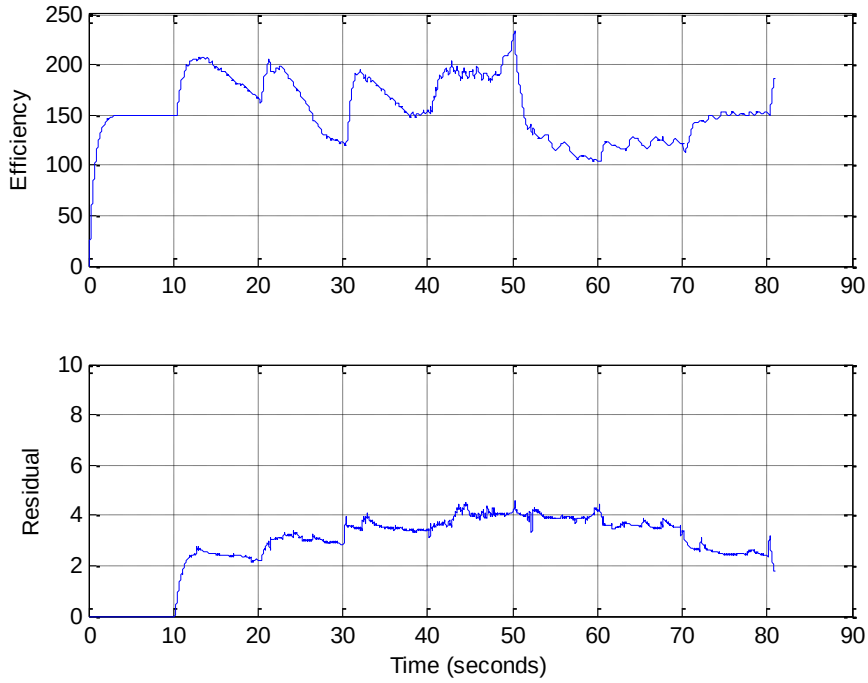

Figure 30: Alternator system efficiency and estimation residual at varying engine RPM under normal condition.

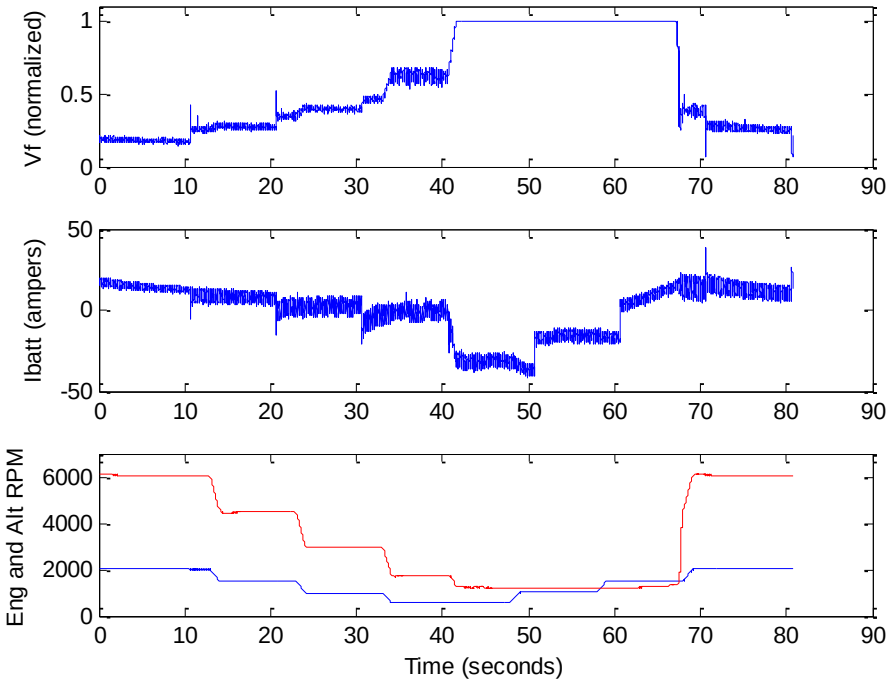

Figure 31: Field voltage, battery current, and alternator RPM vs. varying engine RPM under belt slip condition.

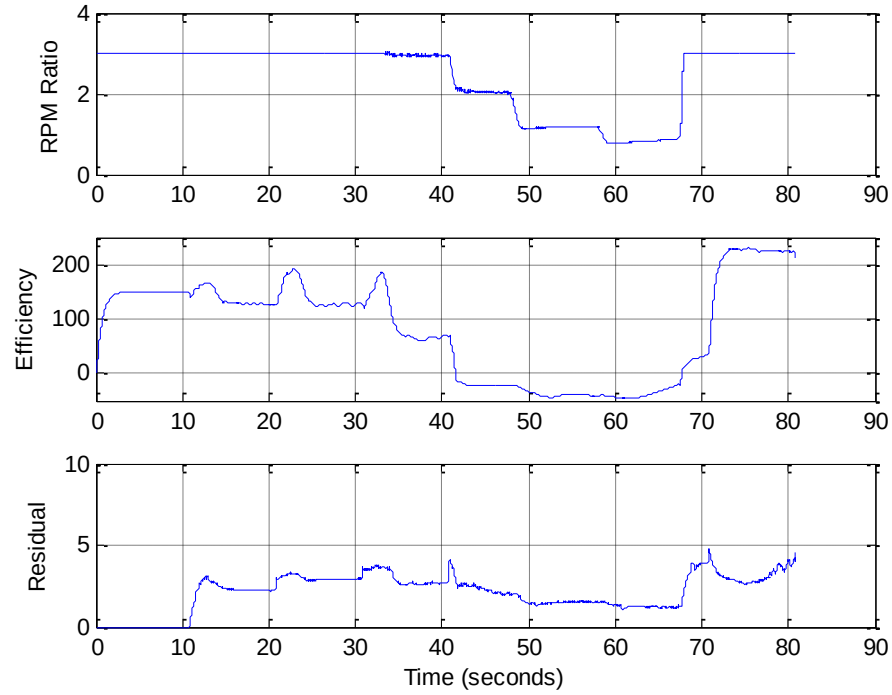

Figure 32: Alternator-to-engine RPM ratio, alternator system efficiency, and estimation residual under belt slip condition at varying engine RPM.

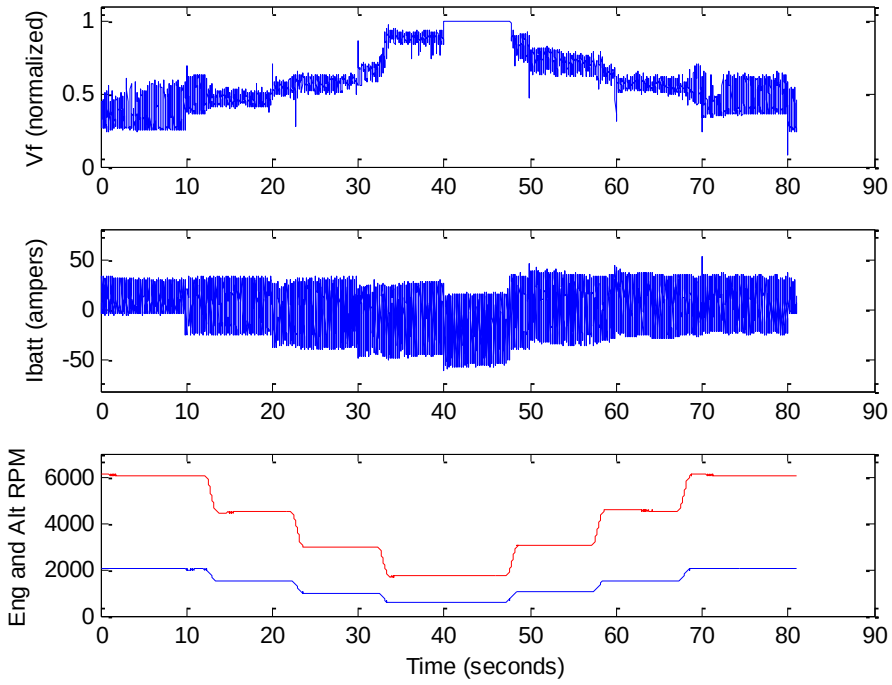

Figure 33: Field voltage, battery current, and alternator RPM vs. varying engine RPM under diode short condition.

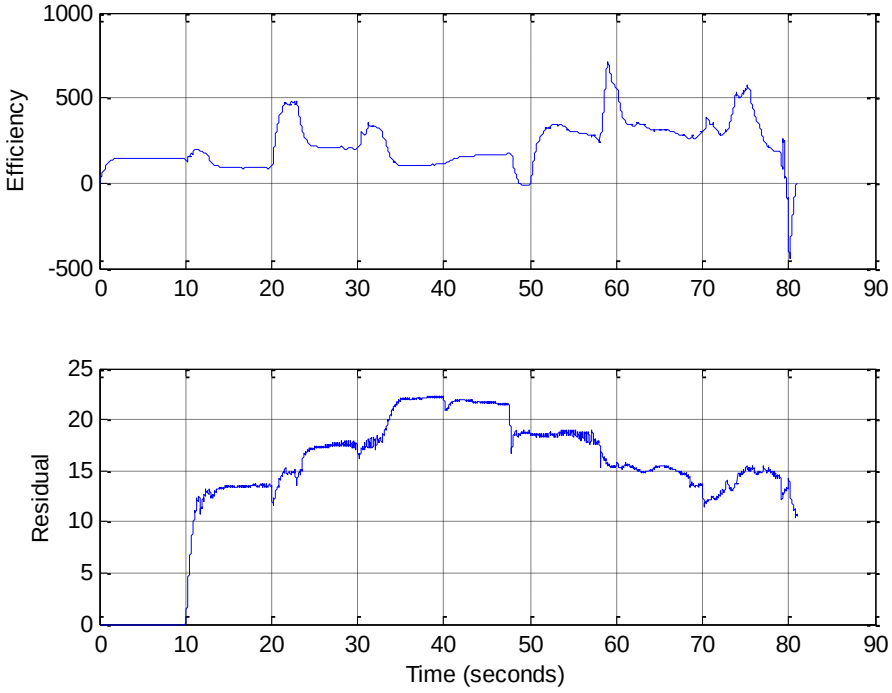

Figure 34: Alternator system efficiency and estimation residual at varying engine RPM under diode short condition.

VII. CONCLUSIONS AND FUTURE WORK

Based on the implementation of the proposed automotive SOH monitoring method on an experimental EPGS system test bench and after examining the real-time algorithm validation results, the following conclusions have been reached:

1. By using a mathematical model characterizing the dynamic relationship between battery current and alternator filed voltage duty cycle under normal operating conditions, the proposed model-based state-of-health (SOH) monitoring method is capable of estimating a key model parameter that represents the current generation efficiency of the alternator system.

2. This parameter allows the timely detection of faults related to the alternator system, among them, slip of the drive belt and a diode short in the alternator rectifier.

Directions for future research work are:

1. Implementation of the alternator system fault diagnosis algorithm on a test vehicle for further robustness analysis.

2. Integration with the battery SOH monitoring method developed in [12] for complete monitoring of the state of health of the automotive EPGS system.

REFERENCES

[1] M. Blanke, M. Kinnaert, J. Lunze, and M. Staroswiecki, *Diagnosis and Fault-Tolerant Control*. Springer, Berlin, 2006.

[2] R. Bosch GmbH, *Automotive Electric/Electronic Systems*. Bentley Publishers, 4th edition, 2004.

[3] D. S. Chen, *Sliding Mode Observers for Automotive Alternators, Ph.D. Dissertation*, The Ohio State University, 1998.

[4] J. Chen and R. J. Patton, *Robust Model-based Fault Diagnosis for Dynamic Systems*. Kluwer Academic Publishers, London, 1999.

[5] A. Emadi, M. Ehsani, and J.M. Miller, *Vehicular Electric Power Systems. New York: Marcel Dekker*, 2004.

[6] J. J. Gertler, *Fault Detection and Diagnosis in Engineering Systems*. Marcel Dekker, New York, 1998.

[7] S. Haykin, *Adaptive Filter Theory*, Upper Saddle River, N.J. :Prentice Hall, 1996.

[8] R. Isermann. *Fault-Diagnosis Systems: An Introduction from Fault Detection to Fault Tolerance*. Springer, Berlin, 2006.

[9] W. Li, C. Suozzo, S. Onori, and G. Rizzoni, "Experimental calibration and validation of fault diagnosis of automotive electric power generation system'" *Proceedings of ASME 2008 Dynamics and control Conference*, Ann Arbor, Michigan, pp. 1317-1324, 2008.

[10] E. Meissner, G. Richter, "Vehicle electric power systems are under change! Implications for design, monitoring, and management of automotive batteries," *Journal of Power Sources*, no. 95, pp. 12-23, 2001.

[11] A. Scacchioli, P. Pisu, and G. Rizzoni, "Hierarchincal model based fault diagnosis for an electrical power generation storage automotive systems," *Proceedings of the 26th American Control Conference*, New York City, NY, pp. 2991-2996, 2007.

[12] X. Zhang, R. Grube, K. Shin, M. Salman, and R. S. Conell, "Parity-relation-based state-of-health monitoring of lead acid batteries for automotive applications," *IFAC Control Engineering Practice*, 2010 (in press).

[13] X. Zhang, H. Uliyar, L. Farfan-Ramos, Y. Zhang, and M. Salman, "State-of-Health Monitoring of Automotive Electric Power Generation and Storage Systems: a Preliminary Study," GM R&D Technical Report, CL-09-26-ECI.

[14] X. Zhang, H. Uliyar, L. Farfan-Ramos, Y. Zhang, and M. Salman, "Fault diagnosis of automotive electric power generation and storage systems," *the 2010 IEEE Multi-conference on Systems and Control* , Yokohama, Japan.